HORIZON 2020

RESEARCH INFRASTRUCTURES

H2020-INFRAIA-2014-2015

INFRAIA-1-2014-2015 INTEGRATING AND OPENING EXISTING NATIONAL AND REGIONAL RESEARCH INFRASTRUCTURES OF EUROPEAN INTEREST

ENSAR2

EUROPEAN NUCLEAR SCIENCE AND APPLICATION RESEARCH 2

GRANT AGREEMENT NUMBER: 654002

DELIVERABLE D5.2 – CLARIFYING AND ADAPTING NUCLEAR CONCEPTS TO THE MEDICAL FIELD

Version: 3.1
Author: G. Magrin, P.G. Thirolf
Date: 24.11.2017

PROJECT AND DELIVERABLE INFORMATION SHEET

ENSAR2 Project Ref. №	654002
Project Title	European Nuclear Science and Application Research 2
Project Web Site	http://www.ensarfp7.eu/
Deliverable ID	D5.2
Deliverable Nature	Report
Deliverable Level*	PU
Contractual Date of Delivery	30.11.2017
Actual Date of Delivery	24.11.2017
EC Project Officer	Mina Koleva

* The dissemination level are indicated as follows: PU – Public, PP – Restricted to other participants (including the Commission Services), RE – Restricted to a group specified by the consortium (including the Commission Services). CO – Confidential, only for members of the consortium (including the Commission Services).

DOCUMENT CONTROL SHEET

Document	Title: Clarifying and adapting nuclear concepts to the medical field	
	ID: D5.2	
	Version 3.1	
	Available at: http://www.ensarfp7.eu/	
	Software Tool: Microsoft Office Word 2007	
	File: ENSAR2_Deliverable_5.2	
Authorship	Written by:	G. Magrin, P.G. Thirolf
	Contributors:	NA5 MediNet WP Conveners/Participants
	Reviewed by:	Dr. Brian Jones (KVI-CART)
	Approved by:	

DOCUMENT STATUS SHEET

Version	Date	Status	Comments
V0.1	02.09.2017	For internal review	Introduction
V0.2	05.09.2017	For internal review	Structure update
V0.3	17.09.2017	For internal review	Section 1 drafted
V1.0	09.10.2017	For internal review	Sect. 3 drafted (incomplete)
V1.1	09.10.2017	For internal review	Sect. 2 drafted (incomplete)
V1.2	10.10.2017	For internal review	Conclusion drafted
V1.3	10.12.2017	For internal review	Sect. 3 updated (incomplete)
V2.0	26.10.2017	For internal review	Section 3 completed and partially revised
V2.1	29.10.2017	For internal review	Sect. 2 expanded, Exec. Summary partially

			drafted, text revision, glossary and bibliography revised
V2.2	30.10.2017	For internal review	Updated the Exec. Summary and Subsect. 3.2.2,
V2.3	1.11.2017	For internal review	Minor text corrections
V3.0	17.11.2017	After internal review	Text corrections T1
V3.1	22.11.2017	After internal review	Text/Figure corrections T2

Document Keywords

Keywords	Radioactivity, secondary reaction products, particle therapy, medical imaging, radiation detectors, radiation quality, clinical effects

Disclaimer

This deliverable has been prepared by Work Package 5 (MediNet – Network: Nuclear Physics for Medicine) of the Project in accordance with the Consortium Agreement and the Grant Agreement n°654002. It solely reflects the opinion of the parties to such agreements on a collective basis in the context of the Project and to the extent foreseen in such agreements.

Copyright notices

TABLE OF CONTENTS

LIST OF FIGURES

LIST OF ACRONYMS AND ABBREVIATIONS

Accuray	Company that provides devices for precise radiotherapy (e.g Cyberknife)
ALARA	As Low As Reasonably Achievable: radiation protection guiding principle
APD	Avalanche photo diode
BEAMnrc	SOFTWARE TOOL TO MODEL RADIATION BEAMS (NOW INCLUDED IN EGSNRC)
BEVALAC	Synchro-cyclotron accelerator in Berkeley, the largest ever built single-magnet device of this type, based on the predecessor 'Bevatron' and operated from 1971-1993
BGO	Bismuth germanate (Bi4Ge3O12): scintillation detector crystal material
CERN	Centre Europeen de Recherche Nucleaire
CNAO	Centro Nazionale di Adroterapia Oncologica (Pavia/Italy)
CRT	Coincidence resolving time
CsI	Cesium iodide: scintillation detector crystal material
CT	Computed Tomography is a medical imaging technique using a large series of two-dimensional X-ray images.
Cyberknife	Robot-assisted linear accelerator for radiotherapy
CZT	Cadmium-Zinc-Telluride: semiconductor detector material
D	Absorbed dose is a measure of the energy deposited per unit mass of medium by ionising radiation, and so has the unit Gy.
DICOM	Digital Imaging and Communications in Medicine: It is a standard for storing, handling and transmitting medical imaging
DNA	Deoxyribonucleic acid: molecule that carries the genetic instructions used in the growth, development, functioning and reproduction of all known living organisms
DOI	Depth of interaction: source of parallax error in PET image reconstruction
DosiSoft	Company providing software for radiation oncology and nuclear medicine
DOSXYZnrc	EGSnrc-based Monte Carlo simulation code for calculating dose distributions in a rectilinear voxel phantom and is based directly on the DOSXYZ code developed for the EGS4 code system
DPK	Dose Point Kernel: The dose distribution in water resulting from both scattered photons and secondary electrons set in motion by primary photon interactions at one particular point.
DSB	Double-strand breaks: breaking of both strands of the DNA double-helix
ECG	Electrocardiography: process of recording the electrical activity of the heart
EEG	Electroencephalography: electrophysiological monitoring method to record electrical activity of the brain
EGS	Electron Gamma Shower: Monte-Carlo radiation transport code
ENIAC	Electronic Numerical Integrator and Computer: first entirely electronic universal computer
ENSAR2	European Nuclear Science And Applications: EU-funded Integrating Initiative with the 'Horizon 2020' funding framework of the EU
eV	Practical unit for energy used in atomic and nuclear physics (e.g. for particle beam energy): 1 eV = 1.6x 10^{-19} J
FDG	Fluorodeoxyglucose is a radiopharmaceutical used in PET imaging.
FLUKA	Monte Carlo simulation package for the interaction and transport of particles and nuclei in matter. FLUKA has many applications in particle physics, high energy experimental physics and engineering, shielding, detector and telescope design,

	cosmic ray studies, dosimetry, medical physics, radiobiology.
GATE	Geant4 Application for Tomographic Emission: (open source) simulation toolkit dedicated to numerical simulations in medical imaging and radiotherapy.
GHz	1 billion Hertz (oscillations per second)
GPU	Graphics Processing Unit
GSI	Gesellschaft für SchwerIonenforschung – Centre for Heavy Ion Research located at Darmstadt, Germany
Gy	Gray is the name of the special unit of absorbed dose of ionising radiation, i. e. the absorption of one joule of ionising radiation by one kilogram of matter. 1Gy = 1 J/kg = 1 m^2/s^2
HDR	High Dose Rate
HSG	Human salivary gland
H2AX	Family of genes coding for the histone H2A. In humans and other eukaryotes, the DNA is wrapped around histone-groups, consisting of core histones H2A, H2B, H3 and H4. Thus, the H2AX contributes to the nucleosome-formation and therefore the structure of DNA.
ICRU	International Commission on Radiation Units and Measurements is a standardisation body set up in 1925 by the International Congress of Radiology.
IFJ PAN	Instytut Fizyki Jądrowej, Polish Academy of Sciences (Krakow/Poland)
IMRT	Intensity-Modulated Radiation Therapy is an advanced type of high-precision radiation therapy technique.
INFN	Istituto Nazionale di Fisica Nucleare, Italy
iPlan	Treatment planning software provided by the company BrainLab
IPNL	Institut de Physique Nucleaire de Lyon (Lyon/France)
ITEP	Institute for Theoretical and Experimental Physics in Moscow (Russia)
KVI-CART	Kernfysisch Versneller Instituut- Center for Advanced Radiation Technology (Groningen/Netherlands)
LaBr3(Ce)	Lantanum bromide (doped with Cerium): scintillation detector crystal material
LEM	Local Effect Model used for the treatment planning system for ion therapy TRiP at GSI and HIT, Germany.
LET	Linear Energy Transfer is a measure of the energy transferred to material as an ionising particle travels through it.
LINAC	contraction of the two words *linear* and *accelerator*
LOR	Line of Response: connecting the registered positions of two diametral emitted positron annihilation photons in a PET scanner
LPC	Laboratoire de Physique Corpusculaire (Clermont-Ferrand/France)
LPSC	Laboratoire de Physique Subatomique et de Cosmologie (Grenoble/France)
LSO	Lutetium Orthosilicate: scintillation detector crystal material
LYSO	Lutetium Yttrium Orthosilicate: scintillation detector crystal material
MCDOSE	A Monte Carlo dose calculation tool for radiation therapy treatment planning
MCNP	general-purpose Monte Carlo N-Particle code that can be used for neutron, photon, electron, or coupled neutron/photon/electron transport (also in use as variant MCNPX).
MCTS	Monte Carlo Track Structure: Monte-Carlo codes for micro- and nanodosimetry
MediNet	Networking Initiative on Medical Physics within the EU-funded ENSAR2 Integrating Initiative

MGH	Massachusetts General Hospital (Boston/USA)
MKM	Microdosimetric Kinetic Model
MMC	Macro Monte Carlo: method that has been developed to improve the speed of traditional Monte Carlo (MC) high-energy electron transport calculations without loss in accuracy.
MRI	Magnetic Resonance Imaging is a medical imaging technique using a powerful magnetic field and radiowaves RF pulse of around 40in the 1-100 MHz range.
NaI	Sodium iodide: scintillation detector crystal material
NIRS	National Institute of Radiological Sciences located at Chiba, Japan
OncoRay	Center for Radiation Research in Oncology (Dresden/Germany)
PARTRAC	established tool for Monte Carlo-based simulations of radiation track structures, damage induction in cellular DNA and its repair
PBK	Pencil Beam Kernel: The dose distribution resulting from scattered photons and secondary electrons set in motion by a single ray of primary photons
PENFAST	A fast Monte Carlo code for dose calculations in photon and electron radiotherapy treatment planning
PET	Positron Emission Tomography is a medical imaging technique using pairs of gamma rays emitted indirectly by a positron-emitting radionuclide.
PET-CT	Positron Emission Tomography and Computed Tomography is a medical imaging device which combines in a single gantry system both a PET and a CT.
PSI	Paul Scherrer Institute: largest research institute for natural and engineering sciences in Switzerland, located in Villigen.
PMT	Photomultiplier tube
PTCOG	Particle Therapy Cooperation Group
RBE	Relative Biological Effectiveness is defined as the ratio of a dose of a reference radiation quality to the dose of the test radiation quality required to cause the same biological level of effect, all other conditions being the same.
RF	Radiofrequency (accelerator property, ca. 100 MHz for typical medical cyclotron accelerators)
SHIELD-HIT12A	Monte Carlo particle transport program which is modified for heavy ion particle therapy.
SiPM	Silicon photomultiplier
SOPB	Spread-Out Bragg peak is an overlap of several pristine Bragg peaks at staggered depths.
SPECT	Single-Photon Emission Computed Tomography
TLE	Track Length Estimator
TOF	Time of flight
TOF-PET	Time-of-Flight Positron Emission Tomography
TPS	Treatment Planning System used in radiation therapy for planning the doses in the tumour and the surrounding healthy tissue (critical organs).
VMC, VMC++, XVMC	Family of Monte-Carlo simulation codes used in external beam radiotherapy, known to be a very accurate and efficient
keV,MeV, TeV, ps	Prefix letters together with a unit denote an abbreviated order of magnitude: keV(kilo-eV): 10^3 eV, MeV (Mega eV): 10^6 eV, TeV (Tera eV): 10^{12} eV, ps (pico second): 10^{-12} s

EXECUTIVE SUMMARY

In the public discussion and perception often an antagonism is constructed between basic and applied research, with priority granted to the latter due to its allegedly higher societal impact. However, in general and in particular in physics, in most cases applications with high societal benefit emerged only after extensive and ground-breaking basic research. With this document the community of the MediNet Networking Activity within the ENSAR2 Integrating Initiative provides information to the general public on the interplay between underlying (nuclear) physics concepts and their translation and application into the medical field. Therefore the scientifically interested layman is the targeted addressee of the present document, which is organized in the following way:

After the introduction the text follows the structure of the MediNet networking activity, which rests on two pillars: the first one (called 'Task 1') dedicated to research on radiation detection instrumentation mainly aimed for application in particle therapy (although with strong synergies into the field of diagnostics), while the second pillar ('Task 2') focuses on nuclear tools for ion beam therapy.

The introduction presents broad scope of physical concepts with direct applications in the medical field, considering historic, conceptual and technological aspects. Amongst these concepts those from nuclear physics have gained a prominent position both in diagnostic and therapeutic applications, e.g. via the application of nuclear decay products (e.g. positron annihilation photons) serving for imaging purposes. Even an advanced concept like the nuclear spin can be exploited for high-precision imaging. Apart from basic physical concepts also technological developments from the nuclear field, like detector technology and particle accelerator science has gained tremendous importance in the medical field over the past decades. Translation of basic concepts into practical medical applications finally means commercialization, based on a cross-fertilizing interplay between academia and industry. In the present document a special focus is laid on particle-based tumour therapy, which is the overarching topic that unites the interests of the almost 30 research groups from 13 European countries that form the MediNet networking activity. The general introduction is followed by an overview of the concept of particle therapy, both from a physics perspective as well as in view of its historic development since first being introduced about 70 years ago. In the subsequent section related to the activities of members of Task 1, nuclear-related messengers for medical imaging particle therapy and diagnostics are presented, considering the concepts of radioactive decay, secondary (charged particle) nuclear reaction products and finally also technological aspects of exploiting synergies of detector developments in the nuclear and medical field. The following section is related to the activities of Task 2. The focus is on some fundamental physics concepts that are transformed central tools to perform ion-beam therapy. The topics discussed include: dosimetry and its translation to biological targets, Monte Carlo simulations to guide the interpretation of biological effects and therapy parameters, the use of the stopping-power concept to characterize the component the radiation in terms of their different effectiveness on the cells, the description of the interaction of the radiation with the matter at biological significant (micrometric) sizes, and the challenges of adapting and controlling the irradiation parameters to ensure the highest therapeutic outcomes.

The documents ends with general concluding remarks.

INTRODUCTION

A large number of ideas, generated from the work of the pioneers of physics disciplines, embrace the field of medicine or more generally human well-being. The research fields of basic physical concepts applied to health are numerous, to name just a few: optics is widely used for microscopy and the concept of total reflection of optical fibers is the base of endoscopy; laser technology is applied in ophthalmology and eye surgery; time resolved electrical current detection is the base of electrocardiography, ECG, and electroencephalography, EEG; studies of mechanics innovations allow the best performances of prosthesis and are the bases, in sport medicine, for subject-specific trainings; mass spectrometry is a key element in the research of biomarkers for cancers.

One of the most prolific interactions between physics and health concerns nuclear physics. Already back in the year 1895, the discovery of X-rays and the density-dependent absorption of electromagnetic radiation was announced by W.C. Röntgen, starting the era of medical imaging. This field became richer and richer during the years, adding more techniques as well as a variety of diagnostic applications. Positron-electron annihilations led to PET (positron emission tomography), single photon emission of specific radioisotopes led to scintigraphy and SPECT (single photon emission computed tomography), and magnetic resonance detection led to MRI (magnetic resonance imaging).

Considering, in this framework, accelerator technology as part of the nuclear field –at least historically the advances in the two fields go together not only because they frequently shared the same scientific goal, but also because they are physically developed under the same roof—one can recognize how this field of research has an emblematic (and very successful) role for enhancing human health, e.g via X-ray Computed Tomography. Today radioisotopes are produced with accelerators and converted, in the same facilities, to radiopharmaceuticals for diagnostic and therapy to be sent to medical centers nearby. Electron accelerators evolved from the first X-ray tubes to the modern linac (the term is the contraction of the two words *linear* and *accelerator*) which, developed specifically for photon therapy, are compact and can move 360 degrees around the patient.

The Bethe-Bloch equation is a fundamental tool for describing the energy lost by charged hadrons (protons, ions, pions) when crossing a medium and it has wide implications in experimental physics. Its use in the framework of health is also large – involving prevention, diagnostics, and therapy – and a peculiarity is that in the two fields of physics and health the related physical quantity has assumed two different names: linear electronic stopping power for the first, unrestricted linear energy transfer for the second.

From the Bethe-Bloch equation one can deduce how the energy of charged particles is deposited when penetrating a medium: the curve that describes the energy deposited has a characteristic shape, the so-called Bragg curve, which has a very distinctive characteristic of reaching its maximum (the so-called Bragg peak) at the very end of the path of the particle, just before stopping. Already in 1946, Robert Wilson recognized how this behaviour could be very advantageous for cancer therapy if one wants to reach tumors that are located deep inside the body of the patients, formally starting proton therapy and ion-beam therapy also known as hadron therapy. The tumor will receive the peak energy (which will result in tumor cell death), while the more superficial tissues will receive less energy (with large probability for the cells to survive).

In the framework of ion-beam therapy many nuclear research centers were and are the indispensable key for study and improving the performance. The first was Lawrence Berkeley Lab in California, where the first treatment with protons was performed in 1954. More recently, several nuclear research centers (including, among

others European facilities in Uppsala, Clatterbridge, Orsay, Nice, and Louvain-la-Neuve) are linked to successful stories, where not only the nuclear physics concepts were adapted for the use of cancer treatment, but the facilities themselves hosted treatment irradiation rooms. In this transition phase an important role was played by the Swiss Center of PSI, Paul Scherrer Institute, in Villigen, where for the first time a small proton beam of a few millimeters diameter (the so-called pencil beam) was moved to cover with the Bragg peak the full tumour instead of a broad and less precise beam. Several centers represented today in the MediNet network gave essential contributions to the development of hadron therapy, such as GSI in Darmstadt (where more than 400 patients were treated for the first time with scanned carbon-ion beams and where the first European clinical center for proton plus carbon ions was developed), INFN in Catania (which hosts in its laboratories a room for the treatment of ocular melanoma with protons), IFJ PAN in Krakow (which, starting with a room for eye treatment, is now hosting a complete facility based on a commercial cyclotron), Dresden (where the OncoRay –Center for Radiation Research in Oncology was built in close cooperation with the research center Helmholtz-Zentrum Dresden-Rossendorf), KVI-CART in Groningen (where a formerly exclusive atomic and nuclear physics research center now provides also research and training capabilities in the medical physics field in support of one of the upcoming new proton centers in the Netherlands being built in Groningen), and the long term effort of French research institutes, including MediNet participants LPC Clermont-Ferrand, IPNL Lyon and LPSC Grenoble, to promote national centers for hadron therapy within the framework of France Hadron.

Challenging aspects of the adaptation of nuclear concepts to the medical field concerns what can be defined as commercialization. In order to translate basic concepts from nuclear physics to the medical sector, a bridging process must be put in place to handle various practical aspects:

- Adaptation of scales from the atomic level to microscopic or macroscopic levels
- Adaptation of the nuclear physics concepts to various applications and complexities –for instance the density-dependent absorption of electromagnetic radiation that is used today in application is very similar to what was originally done by Röntgen (dentist's X-rays or mammography) as well as very complex and challenging integrations (computer tomography, CT, also in combination with PET and MRI)
- Adaptation of conditions from experimental physics environment (i.e. well-controlled experimental conditions and flexibility in time and space to perform measurements) to severe restrictions imposed by the clinical settings (conditions in the human body that cannot be simplified, rapidity of treatment, and safety aspects)
- Adapt interplay factors (i.e. adapt the typically unambiguous, deterministic correlations between ideally two physical parameters to the far more complex systemic scenario found in the medical field). Based on the specific expertise of research fields represented in MediNet, this document will focus on selected research topics within the network (see below) with two main scopes:
- Clarifying the physics concepts underlying the various aspects of nuclear physics translated into the medical field, in particular radiation therapy, while focusing on an audience of non-experts with a general scientific background (the model recipients being students at the end of their high school curriculum, ready to enter university).
- Describing the major challenges (see below) concerning the adaptation to medical needs and what is presently pursued as research lines in particular within MediNet, including the optimization of existing tools and novel developments.

SECTION 1: OVERVIEW OF THE CONCEPT OF PARTICLE THERAPY FOR TUMOR TREATMENT

Tumor treatment with charged particles (protons, ions) is intimately linked to the nuclear physics concept of specific energy loss. This describes the continuous reduction of the kinetic energy of fast charged particles when they traverse matter, until finally coming to rest after a distance which is called their stopping range. From the nuclear physics perspective, the specific energy loss is induced by the interaction of the impinging particles with the electrons of the stopping medium ('electronic stopping'). Characteristic dependencies on the properties of the fast particles include an increase of the deposited kinetic energy with the square of the nuclear charge (number of protons in the nucleus) of the fast particles and a decrease of the energy loss inversely proportional to the (square of the) velocity of the protons or ions (in the energy range of practical relevance for tumor treatment). Thus slower particles deposit more kinetic energy in the stopping medium and the energy loss of slowing-down particles increases towards the end of their trajectory, thus depositing a maximum of energy in a narrow region close to their endpoint in what is called the 'Bragg peak'. Thus it is possible to deposit a high dose in a well-defined volume of the stopping medium, while sparing the surrounding volume, in particular the region behind the Bragg peak, from unwanted dose deposition. The complete energy-dependent behavior of the specific energy loss is described by the so-called Bethe-Bloch equation, which allows one to calculate the depth-dose distribution with high accuracy. The described behavior of charged particles traversing matter is fundamentally different from photon attenuation in matter. Here the deposited energy (and thus the applied dose to the medium) is decreasing exponentially along the photon track (after some buildup range close to the surface). From the perspective of tumor treatment this implies that dose deposition in healthy tissue in front of and behind the tumor volume is unavoidable with all its negative side effects. On the other hand, varying the energy (and position) of the charged-particle beam (and thus the position-dependent stopping range) allows for a highly conformal dose deposition across the full tumor volume. In this case the rather sharp Bragg peak in the case of monoenergetic protons or ions is modulated into a so-called 'spread-out Bragg peak (SOBP)'. In X-ray radiotherapy, conformal dose deposition in the tumour volume can be achieved by irradiating the tumour target volume from different directions by rotating the radiation source (the so-called gantry) around the patient in order to minimize the dose given to the healthy tissue (IMRT: image-guided radiotherapy).

These features are displayed in Figure 1, where a comparison of the depth-dose curve for photons (X-rays) and protons (monoenergetic and polyenergetic to form the SOBP is shown.

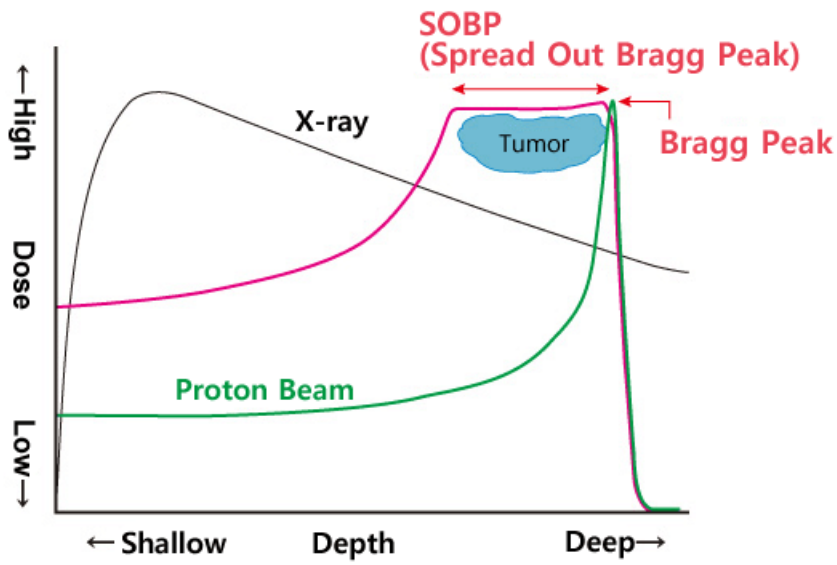

Fig. 1: Depth-dose curves for photons (X-rays) and protons (monoenergetic: green, polyenergetic: purple), indicating the different dose deposition behavior of photons and charged particles when traversing matter. The 'spread-out Bragg peak' can be tailored to provide a highly conformal dose deposit to the tumour volume, thus largely sparing surrounding healthy tissue from unwanted dose deposition. In the case of X-ray radiotherapy, conformal dose deposition can be achieved by irradiating from different directions via a rotating gantry (see text).

The proposal of exploiting the favorable properties of heavy charged particles for cancer treatment was first suggested by Robert R. Wilson, at the time working at Harvard University. Patient treatment with proton, deuteron and helium ion beams in 1954 at the Radiation Laboratory in Berkeley, was performed employing the existing synchro-cyclotron accelerator. Europe followed three years later in 1957, when the first patients were treated with proton beams at the Gustaf-Werner-Institute in Uppsala (Sweden). From the 1960's to the mid 1980's tumour treatment with charged particle beams was hosted exclusively at research centers in the US, Europe and Japan with accelerator facilities developed and predominantly used for nuclear physics research. Specific beamlines and treatment rooms had to be adapted and added according to the needs of patient treatment. Nuclear research facilities treating patients comprised the Harvard Cyclotron Laboratory (USA), The Gustaf-Werner Institute in Uppsala (Sweden), the Paul-Scherrer-Institute in Villigen (Switzerland), the Institute for Theoretical and Experimental Physics (ITEP) in Moscow (Russia), the Joint Institute of Nuclear Research in Dubna (Russia), the Leningrad Institute of Nuclear Physics in Gatchina (Russia), the National Institute of Radiological Sciences in Chiba (Japan), the University of Tsukuba (Japan) and the National Accelerator Centre in Johannesburg (South Africa), nowadays named iThembaLABS. Having thus laid the foundations for particle therapy according to the principle of 'bringing the patient to the accelerator', a new era in particle therapy started in the 1990s with the construction of dedicated accelerators in hospital-based clinical treatment centers, thus 'bringing the accelerator to the patient'.

Obviously, particle therapy intimately relies on the availability of suitable particle accelerators. Here another nuclear concept found its way into the medical field, since the historical development of accelerator technology was mainly driven by the needs of subatomic physics research. At the time of Wilson's seminal proposal to use heavy charged particles for tumor treatment, accelerators capable of providing beams with the required energies to reach any location in the human body (ca. 230 MeV for protons and ca. 400 MeV per nucleon for carbon ions) did not even exist. After the invention of the synchro-cyclotron (a circular particle accelerator based on rapidly oscillating high-frequency voltages with decreasing radio-frequency to compensate for relativistic effects), independently by Veksler in Russia and McMillan in the US [Veksler 1944, McMillan 1952], proton and helium beams could be accelerated to energies required to reach also deep-seated tumours. Still the first patient treatment with protons in 1954 was performed at the 188 inch (4.67 m) synchro-cyclotron in Berkeley (the BEVALAC, the largest ever built single-magnet device of this type), which was motivated by fundamental high-energy particle-physics studies. Translation of the (sub-) nuclear motivated particle accelerator concept into the medical field took until 1961, when the first dedicated proton therapy facility started operation at the 160-MeV synchro-cyclotron at Harvard University. Since then continuous optimization of dedicated medical accelerators proceeded. A major step forward was again achieved by a breakthrough in particle-physics driven accelerator technology, namely the development of the heavy-ion synchrotron. Patient treatment with ions from helium to argon was pioneered at the Berkeley Bevalac accelerator facility in the 1970s and 1980s, leading – after the decommissioning of the Bevalac accelerator in 1993 - to an extensive research program on carbon-beam therapy mainly in Japan (NIRS/Japan) and Europe (GSI/Germany). Finally, the translation of the initially nuclear- or particle-physics driven accelerator technology into dedicated medical therapy application was boosted by commercialization and competition between different vendors.

When it comes to delivering the particle beam to the patient and the identified tumor volume, at present the above described beneficial properties of particle therapy with a highly conformal dose deposited to the tumor volume cannot be fully exploited. The sharp Bragg peak necessitates an accurate and reliable positioning of the endpoint of the proton range inside the tumor volume and in safe distance to potentially nearby critical organs-at risk. However, the proton or ion range in tissue is associated with considerable uncertainties in the exact position

of the distal dose gradient arise from (a) organ motion, (b) setup and anatomical variations, (c) dose calculation approximations and (d) biological considerations, calling for safety margins around the tumor volume to be considered in the treatment planning process. At the Massachusetts General Hospital (MGH, Boston/USA), treatment planning assumes an uncertainty in the proton beam range of 3.5% of the particle range plus an additional 1 mm. Other centers follow similar margin recipes. Reducing these uncertainties would allow for a reduction of the treatment volume and thus allow a better utilization of the advantages of protons or ions by more efficiently sparing healthy tissue. Figure 2 illustrates the ratio between tumor volume and surrounding safety margin during particle therapy with the analogy of an orange: removing the 5 mm thick outer layer results in a reduction of the remaining volume by a factor of two, i.e. the volume of the outer layer equals the volume of the core orange [Verellen 2007].

Fig. 2: Analogy to illustrate the ratio between irradiated (orange-sized) tumor volume and the volume of a 5 mm safety margin: the volume of the peeled-off outer layer of the orange equals the one of the core orange [Verellen 2007].

Precise particle beam range monitoring, which forms part of the MediNet research activities via R&D on related instrumentation [Hueso-González 2015, Bisogni 2017, Roellinghoff 2014, Richter 2016], thus can assist the goal of enabling full exploitation of particle therapy capabilities by reducing the amount of irradiated healthy tissue.

SECTION 2: NUCLEAR MESSENGERS FOR MEDICAL IMAGING IN PARTICLE THERAPY AND DIAGNOSTICS

2.1 Radioactive Decay

Radioactive decay represents a key nuclear concept that serves as a basis for widespread applications in the medical field. Radioactive decay corresponds to the spontaneous transformation of an unstable nucleus into another nucleus. The total mass energy balance in such a reaction is positive, so that emitted particles carry out kinetic energy. The various decay modes are:

- β^- emission: inside the nucleus, a neutron transforms into proton: n → p + e- + $\bar{\nu}_e$, where $\bar{\nu}_e$ is an antineutrino. The total kinetic energy released K is shared between the electron and the antineutrino. Therefore, the energy spectrum of the electron β^- extends up to the maximum value K (of the order of a MeV).

- β^+ emission: similar to β^- emission, but it corresponds to the transformation of a proton into neutron: p → n + β^+ +ν_e, where ν_e is a neutrino. The particularity of the emitted β^+ particle, called positron and being the antimatter partner of the electron, is that, within matter, it will annihilate by combination with an electron, giving rise to two gamma rays of equal energy emitted at 180°, when the annihilation occurs at rest. Indeed, this annihilation occurs

mostly after slowing down of the positron, which induces a spatial shift between the location of the β^+ decay and the location of the annihilation.

- α emission: the nucleus emits an α particle, that corresponds to an ^{4}He nucleus. The kinetic energy of the particle is of the order of a few MeV, which represents a range of less than 50 µm in solid or liquid matter.

- electron capture from a bound electron by the nucleus: $p + e^- \rightarrow n + \nu_e$, This reaction does not lead directly to a measurable product, but the electronic rearrangement of the atom leads to the emission of Auger electrons and/or x-rays, since the captured electron originates in general from the most inner shell.

- spontaneous fission of a heavy nucleus into two lighter fragments.

- gamma emission of an excited nuclear state is not per se a radioactive decay, since the nucleus is unchanged.

- rare decay modes like proton emission, neutron emission or cluster emission do exist as well.

All these processes occur naturally, they obey rules of probabilistic decay probability: $dN=-\lambda N$, where N is the number of unstable nuclei, -dN is the decay rate per unit time, and λ is the radioactive decay constant. One generally characterizes the decay rate by means of the half-life $t_{1/2}$ of the nucleus, where $t_{1/2} = \ln 2/\lambda$. For a given amount N of a radioactive nucleus, the activity A (number of decays per second) is $A = -dN = \lambda N$.

The production of radioisotopes is performed by means of nuclear reactions, either from natural environment: hot nuclear matter in stellar or astrophysical media, or artificially by means of accelerators or nuclear reactors.

Radioactivity in the medical domain is used for two main purposes: radiotherapy and imaging:

- **Radiotherapy** with radioactive isotopes is performed either by introducing a source close to-, or inside the planned treatment volume by means of a catheter (brachytherapy) or by injecting the radioelement inside targeting molecules (targeted therapy with alpha or beta emitters). Brachytherapy uses mainly gamma emitters like ^{192}Ir or ^{125}I. Recent developments of High Dose Rate (HDR) brachytherapy make use of ^{60}Co sources. Vectorized radiotherapy is an emerging modality where the radioisotope is transported by a vector molecule targeting the organ (for instance ^{131}I is fixed inside thyroid). Figure 3 illustrates how emitted radiation may transfer more or less energy at various distances: alpha particles deposit typically 50-200 keV/µm, and have a range of <100 µm. β particles are fast electrons, their LET is typically 0.1-1 keV/µm and the extension of the volume of energy deposition is roughly 1-10 mm. Auger electrons are emitted after inner-shell vacancy is created, for instance by means of electron capture. The amount of Auger electrons increases for heavier atoms. Auger electrons are emitted more or less isotropically, with energy of the order of ~10 eV, their LET is in the range 4-25 eV, and their range is quite small (0.5 µm), which makes them quite efficient for killing a single cell surrounding the radioisotope.

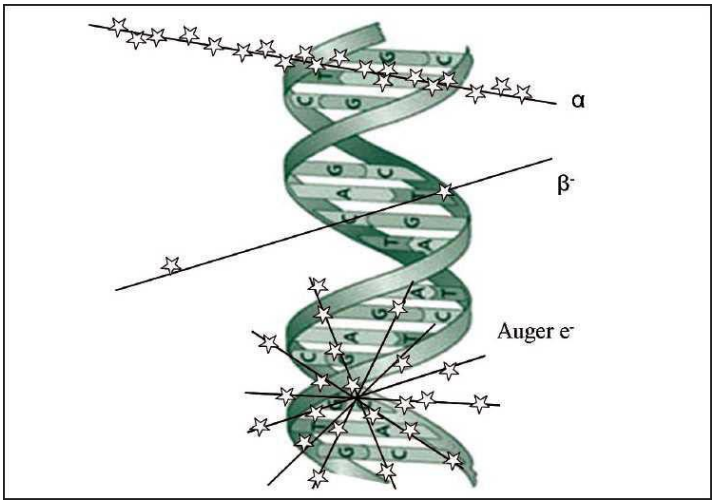

Fig. 3: illustration of energy deposition by α, β particles and Auger electrons at the scale of a DNA helix.

Although this is out of the scope of this report, these techniques enable high dose gradients, and detailed local dosimetry is a crucial question addressed to physicists. In particular, quantitative imaging of the radioisotope distribution either before the treatment, or during the treatment, may bring precious information for the optimization of the treatment quality.

- **Nuclear imaging** consists, after injection of a radioisotope into the vascular system of a patient, in observing externally the decay products, namely gamma rays, that are expected to emerge from deep inside. The imaging of the location of disintegrations provides an image of the organs where the radioisotopes fixed preferentially. The radioisotopes are therefore currently embedded into targeting molecules, like FDG. Two kinds of radioisotopes are of interest here: β+ emitters and γ emitters (that are not necessarily emitting only γ rays). Indeed, only γ rays are expected to be transported throughout matter without being significantly deviated. 3D imaging of γ rays requires the acquisition along several planes of observation, and therefore it is often performed by means of computed tomography, i.e. the detectors are rotated around the region of interest. Positron Emission Tomography (PET) has the particular advantage that two 511-keV γ rays are emitted back-to-back when a positron annihilates close to the nucleus decay point (or a few millimeters away). Thus, the detection of the two photons in temporal coincidence with position sensitive detectors enables one to reconstruct the Line of Response (LOR) without collimation. The principle is illustrated in Figure 4.

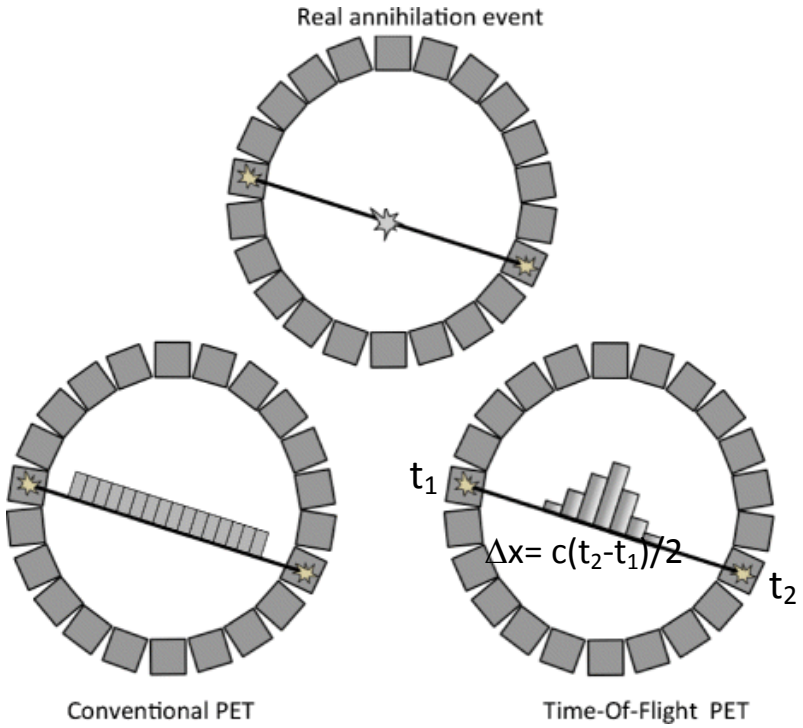

Fig. 4: Illustration of PET photon detection principle. With conventional PET, the annihilation event has a uniform probability along the Line of Response (LOR). Time of Flight enables one to reduce the probability along a segment of length $\Delta X = c\Delta t/2$, where Δt is the coincidence timing resolution, and c the speed of light.

The image of the radioisotope distribution is obtained by reconstruction using a large number of LORs that are intersecting on the emission points. Thanks to a very low background (due to fortuitous coincidences or to scattering of photons) PET provides a highly sensitive detection of the radioisotopes, with millimetric spatial resolution. The use of Time-of-Flight to reduce the time-coincidence window enables one to reduce the background, and thus enhance even more the sensitivity and reduce examination times or injected doses (see Fig. 4).

Besides PET, Single Photon Emission Computed Tomography (SPECT) is used for radioisotopes emitting a single photon. Therefore, one needs a directional detector, either with collimation set in front of a position-sensitive detector, or with the technique of Compton imaging. Compton cameras are composed of at least two detection stages, where Compton scattering occurs in the first one, and the scattered photon interacts in the second stage [Hueso-González 2014, Krimmer 2015, Polf 2015, Solevi 2016, Thirolf 2016]. Both stages record the interaction position and the deposited energy, which makes possible to define a cone from where the original photon was emitted. A reconstruction strategy is necessary to image the radioisotope spatial distribution (intersections of cones). Although Compton cameras are promising for high energy photons, at present, only collimated cameras are used clinically.

Present related research in MediNet:

Current research performed in the MediNet Networking Initiative in the field of nuclear imaging is oriented toward TOF-PET, multimodal imaging [Marafini 2015, Bisogni 2017] and innovative SPECT with Compton cameras.

TOF-PET is already commercialized by major imaging companies. However, there is still a gap between available time resolutions (400-600 ps) and resolutions of less than 100 ps that would be necessary to reach ~1 cm accuracy along a LOR, and thus almost suppress the reconstruction phase of an image. Such resolution may be achieved with very fast scintillators and electronic readout, or with non-scintillating materials such as resistive plate chambers.

A competing alternative to TOF-PET is the use of three-photon decays that are available for some particular isotopes such as ^{44}Sc, a β^+ and γ emitter. The combination (or integration) of a SPECT with a PET detection device reduces the LOR to a single point, which makes reconstruction useless. Several devices are under construction (e.g. [Thirolf 2016]) that may lead to such a multi-modality.

Compton cameras that were primarily dedicated for online control of particle therapy may be used for SPECT, opening the way to high-energy γ imaging [Fontana 2017].

2.2 Secondary Radiation Imaging

The energy loss of light ions used in particle therapy is dominated by electromagnetic interactions. In spite of that, the nuclear interaction of the beam with the patient tissues has sizeable impact on the dose release pattern. In particular the main effects are:

- Production of lighter and lower-charge secondary fragments with respect to the beam, which move at very similar speeds to that of the primary ion and therefore have a greater range. This effect produces a dose release beyond the Bragg peak (dose tail) that must be taken carefully into account;

- Progressive decrease with the path inside the patient of the percentage of the primary ion (for example ^{12}C) with respect to the produced component of lighter fragments. To quantify this effect, out of a 400 MeV/u kinetic energy carbon beam, 70% undergo nuclear fragmentation and do not reach the Bragg peak ;
- Increasing the lateral distribution of the dose in the material resulting from the contribution of the secondary fragments emitted.

At the energy of interest in Particle Therapy (100-400 MeV/u) nuclear collision can result both in a complete disintegration of both beam and target nuclei (for example, in a head-on collision), or in partial fragmentation. In the case of central collisions, almost all the nucleons of the target and of the projectile can participate in the reaction, with the production of high multiplicity of fragments. However, for geometric reasons, the most frequent nuclear reactions are peripheral collisions, where the beam loses only one or a few nucleons. Usually during this collision the few nucleons interacting belong to the overlapping zone between projectile and target nucleus, and hence both the number of participating nucleons, the energy and the transferred momentum are relatively small. As a result, in the reference system of the laboratory, few fragments are observed, mainly in forward direction, at about the same velocity as the beam. Such particles may derive from the direct overlap of the nuclei or may result from the de-excitation of the projectile after the collision (projectile fragmentation).

Another family of fragment can be observed in these reactions: light particles that have almost isotropic distribution in the lab system. These particles are usually products of the target nuclei de-excitation following collision (target fragmentation).
In general the collision fragmentation process can be described with the two-stage abrasion-ablation pattern that occurs in two different time scales. This model is schematically illustrated in Figure 5.

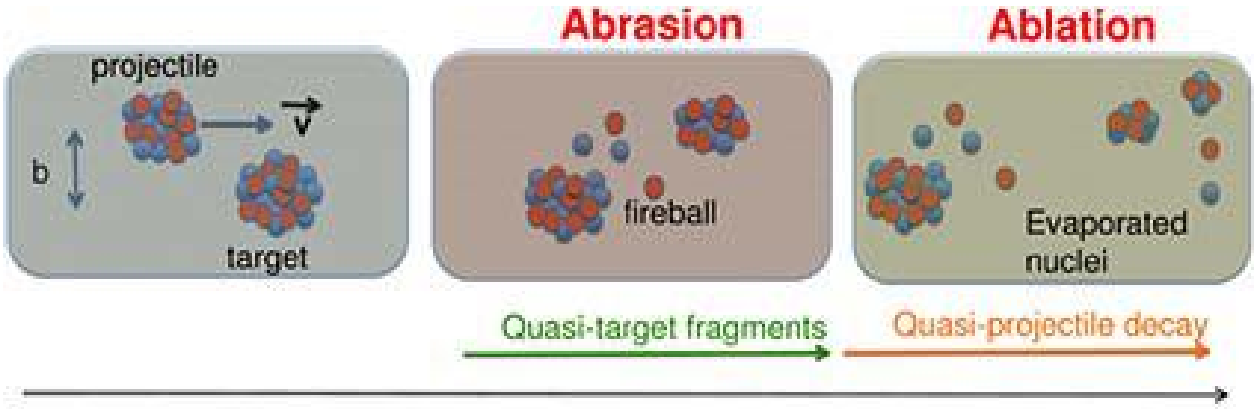

Fig. 5: Abrasion-Ablation scheme of nuclear interactions.

The first stage is called abrasion, when the projectile nucleus strikes the core of the target nucleus, the nucleons inside the overlapping zone (called fireball) interact with each other and are expelled from the bullet and the target. In this stage light particles are emitted. Projectile fragments follow the initial trajectory at about the same initial speed, while the recoil fragments have in general low energies.
In the second stage of the reaction, the ablation phase, the system is thermalized and dissociated due to the evaporation of neutrons, protons and light nuclei. Throughout all the de-excitation phase there is a competition between the evaporation process and the gamma ray emission, or simultaneous breakdown with the emission of intermediate mass fragments.

In general, the fragmentation of the nuclei of the target contributes to a small extent to fragment production in the case of $Z > 1$. On the contrary, in the case of proton beams only the target nuclei can fragment.

Most of the charged fragments produced in the incident beam fragmentation have smaller dimensions than the projectile, but similar speeds. Since the charged particle range scales as A / Z^2, at constant velocity the fragments will deposit part of their energy beyond the beam Bragg peak, producing a tail in the distribution of the dose called fragmentation queue. The angular distribution of these fragments is mainly forward directed, but with a much larger angular diffusion than the multiple scattering lateral diffusion of the primary beam.

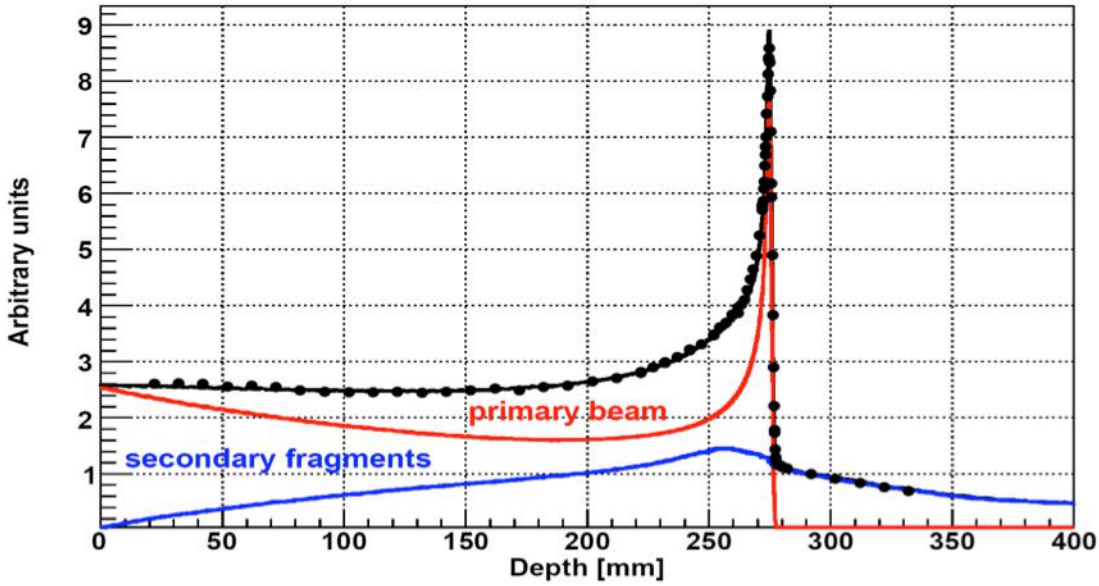

Figure 6: Bragg curve of a 400 MeV / nucleon carbon beam in water. The points represent the experimental data [Haettner 2006] while the continuous lines represent the FLUKA simulation [Mairani 2007].

Figure 6 shows the primary ion contribution to the dose release of a 400 MeV/u carbon beam in water with respect to the one due to the produced fragments. The actual dose distribution along the beam path (black line in Fig. 6) has a very large contribution from the fragments produced in nuclear interactions (blue line). The impact of these effects can increase depending on the depth of penetration, or of the beam energy. For example, for a ^{12}C beam of 200 MeV/u, traveling in water, about 30% of primary ions are involved in nuclear reactions and do not reach the Bragg peak, while at 400 MeV/u this fraction increases up to 70%. This modification of the beam composition is partially present also for proton beams: in a proton beam with kinetic energy equal to 150 MeV, only 80% of the primary particles reach the Bragg peak. With proton beams the secondary fragments are due only to the fragmentation of the target and therefore their speed is very small: their range does not exceed a few microns (with the exception of neutrons and light charged particles knocked out close to the beam entrance), and they deposit their energy near the point where the collision occurs.

The study of the secondary charged particles produced in the nuclear interaction of the beam in the patient is of interest not only to take into account the fragment dose in the treatment plan, but also because the secondary particles are the only means to monitor the beam position inside the patient in particle therapy. To this aim new approaches must be developed, taking into account that the energy release of the beam is largely driven by the electromagnetic interactions with the patient, while strong interactions are needed to produce radiation that can escape the patient and allow for an imaging of its source. Three nuclear processes can yield radiation suited for this purpose: production of β^+-emitting nuclei, excitation of nuclei and fragmentation.

Nuclear β^+ decays produce positrons that can be traced exploiting their annihilation with electrons that yield back-to-back 511 keV photon pairs (i.e. exploiting the same technique of a standard PET diagnostics, see previous section). As tissue is mostly constituted of carbon, hydrogen and oxygen, the most likely β^+ emitting isotopes that can be formed are ^{10}C (with a lifetime τ = 28 s), ^{11}C (τ = 29 min), ^{14}O (τ = 102 s), ^{15}O (τ = 176 s), ^{13}N (τ = 14 min). The relative composition depends on the projectile.

The passage of the beam in the patient can also excite the nuclei whose de-excitation generates photons. Since this process is mediated by the strong interaction, it has very short (< 1 ns) decay times and the photons are promptly produced. This prompt radiation is spatially correlated with the beam path and can be detected by means of evolutions of the standard SPECT techniques [Krimmer 2017]. Albeit dominated by the 4.44 MeV and 6.13 MeV lines from $^{12}C^{*}$ and $^{16}O^{*}$ respectively, there is a large continuum spectrum up to almost 10 MeV.

Finally, the production of charged fragments is a process with high cross-section, where either the projectile and the target nucleus or both fragment into charged ions of smaller mass. The understanding of this process is particularly difficult, because the energy regime of interest is relatively low (at the moment of the interaction, projectile energies range between 20 MeV/u and 200 MeV/u) and therefore the strong interactions are particularly difficult to model. During the last decade several measurements have been performed to evaluate the dose contribution to healthy tissues due to the beam production of these fragments, but little or no attention has been paid to the production of the large angle, low ionizing, highly penetrating proton component, that can be exploited for monitoring purposes.

In the last decade a lot of efforts have been focused on the study of the nuclear interaction between the beam and the patient tissue. Each of the secondary particles produced has been measured and in particular the gamma emission, both PET and prompt component, has been explored. Charged particle production as well is in the focus of the physics community, while future experiments are foreseen to further explore the less known neutron production in particle therapy.

2.3 Exploiting synergies of detector developments in the nuclear and medical field

Ever since the beginning of the medical imaging era, with the discovery of X-rays by Wilhelm Röntgen, medical imaging equipment is advanced, at times in a revolutionary fashion, every time a new radiation detector is introduced or evolved in the experimental nuclear physics laboratory. However, more recently, the increased importance of the medical industry led to the development of dedicated materials such as scintillators and semiconductor detectors with medical applications in mind, but these detectors are also useful for basic nuclear experiments. Today new detectors, electronics and algorithms are being put at play, more and more often with the applications in medical imaging in mind, but as it has always been, these new devices are refined, evolved, optimized, reformulated, thanks to intense tests and use in nuclear physics facilities all over the world. The field of medical imaging is vast, and nowadays, thanks to the enormous advances in electronics, informatics and nuclear detectors, it is dominated by fully 3D, tomographic images and it is improving at the fastest pace ever seen. We will restrict this discussion to a few sub-aspects of medical imaging. In the first case, there is nuclear imaging, where a molecule labeled with a radioactive element is tracked inside the body by means of nuclear detectors. When the radioisotope emits single gamma rays and we use them to obtain 3D images, this is single photon emission computed tomography (SPECT). If, on the other hand, the radioisotope emits positrons, we are in the realm of positron emission tomography (PET) imaging. Both emission image modalities are termed functional imaging, or even molecular imaging, because images of particular molecules inside the body are obtained. Secondly, we will discuss conventional transmission X-ray imaging, again in the tomographic version or X-ray CT. Transmission and emission imaging principles are schematically illustrated in Figure 7.

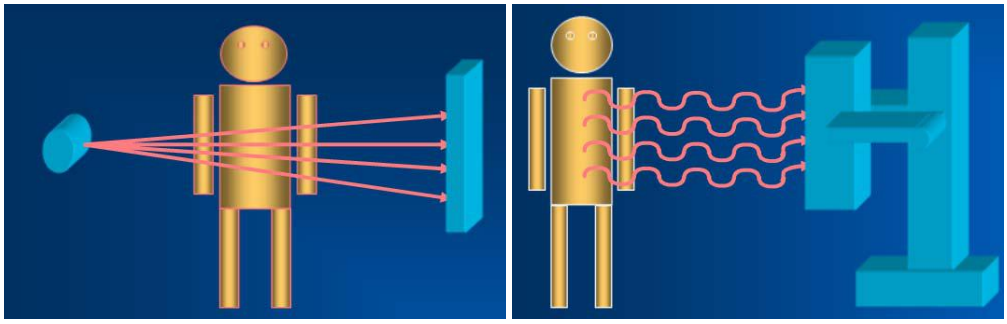

Figure 7: Left: Schematic illustration of (X-ray) transmission imaging. Right: Scheme of (photon) emission imaging (as used in PET and SPECT devices)

SPECT: In this modality, relatively low energy (< 250 keV) gamma rays are emitted by radioactive isotopes (^{99}Tc, ^{201}Tl, ^{67}Ga, ^{111}In, ^{123}I) and detected. These gamma rays can interact with the patient's body before reaching the detector (scatter of the photon), losing some energy and also changing direction. These scattered photons deteriorate the quality of the image. Continuous progress has been made in recent years with the development of new materials with better energy discrimination capabilities, thus allowing for the disentangling of scattered photons from the ones that flew directly from the labeled molecule to the detector. Among these new materials one should mention Cadmium-Zinc-Telluride (CZT), a high energy resolution semiconductor, which also displays a large stopping power capability, and a high efficiency for gamma photon detection. Also, new scintillators, specifically developed with medical imaging in mind, are being developed. These new scintillators substitute with advantage old crystals such as NaI or CsI, which have been in use for the past 70 years and were first introduced for performing basic nuclear spectroscopy. $LaBr_3$(Ce) in particular is suited for SPECT and gamma cameras, as the ones we find in prompt-gamma range verification devices for hadron therapy. Thin, continuous slabs of $LaBr_3$ scintillators, read out by multiple photodetectors, combine high spatial and energy resolution and this is a very active area of research these days, pursued also within the scope of the MediNet networking activity.

Related to SPECT, one cannot forget the so-called 'Technetium problem', arising due to the end of life-cycle of many research reactors, where this isotope was produced, thus causing a shortage of this radioisotope (as well as other isotopes crucial for diagnostics and therapy). Nuclear physicists all over the world are looking for feasible alternatives for its production. For example, accelerator-driven production methods are currently under investigation. If successful, such an approach may allow a more finally distributed and therefore more robust network of production facilities. Nevertheless, maintaining sufficient reactor-based production capacity remains of vital importance until alternative production techniques have matured to the point where they can be used reliably and safely for the production of medical isotopes. Also, alternative isotopes or nuclear imaging technologies are being tested to replace Tc-based SPECT.

PET: This is probably the star among the nuclear imaging modalities at play, and the one experiencing the fastest evolution. In the case of PET imaging, the simultaneous arrival of two annihilation photons, with energy of 511 keV, marks a valid event. Photons involved in PET imaging have a relatively high energy compared to SPECT ones, and thus they have a penetration in the PET detector of the order of 10 mm, which typically is not taken into account when reconstructing the 'Line-of-Response' between the two opposite detectors registering the 511 keV photons. This potential parallax error, which is called 'depth of interaction (DoI) effect' blurs the position of the event and worsens the quality of the PET image (see Fig. 8). This can be alleviated somewhat by using smaller detectors, and this way the spatial resolution of clinical PET scanners has improved steadily, from about 7 mm being commonplace eight years ago, to about 4 mm for the most recent commercial scanners. Even smaller crys-

tals, or alternatively, continuous blocks of detectors together with sophisticated electronics and signal processing in order to attain 3D positioning of the event in the detector, with mm precision, are being used. This way, prototypes and some commercial preclinical and dedicated (brain, breast) PET scanners are achieving spatial resolutions of less than 2 mm, which will probably be translated to most clinical scanners in the following years.

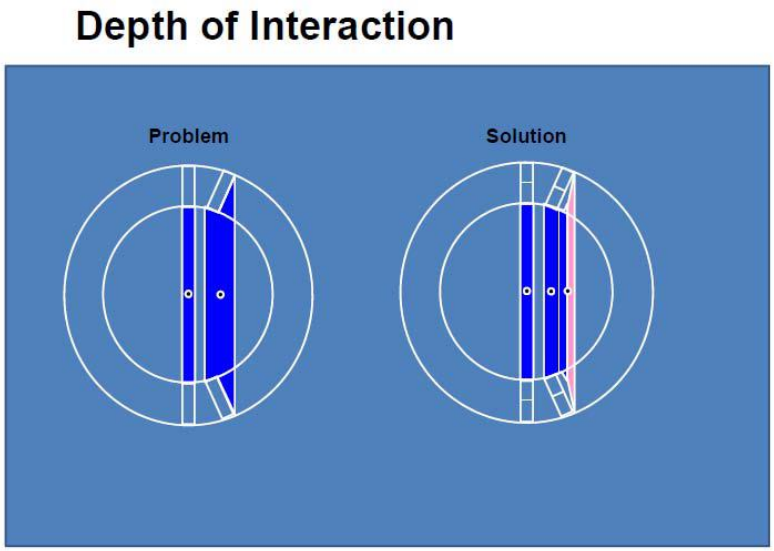

Figure 8: Illustration of the 'depth of interaction (DoI)' effect in PET photon registering.

Due to their good energy and time resolution compared to the traditional PET crystal material (BGO), the new PET scintillation crystals (LSO, LYSO) are being increasingly used on commercial PET scanners. With these new scintillators, the time-of-flight (ToF) difference among the two photons defining a PET coincidence event can be used to increase the signal-to-noise ratio and contrast of the image (see Fig. 9). Most commercial clinical scanners, based on LSO or LYSO crystals, today exhibit a ToF resolution of the order of 400 ps. Clinical PET scanners based upon $LaBr_3$ are beginning their deployment and exhibit ToF resolution values ('coincidence resolving time', CRT) of 250 ps or less. Most certainly CRT values will decrease below 200 ps in the next five years, which would boost by a factor of two the detectability of hot lesions (tumours for instance) in PET images.

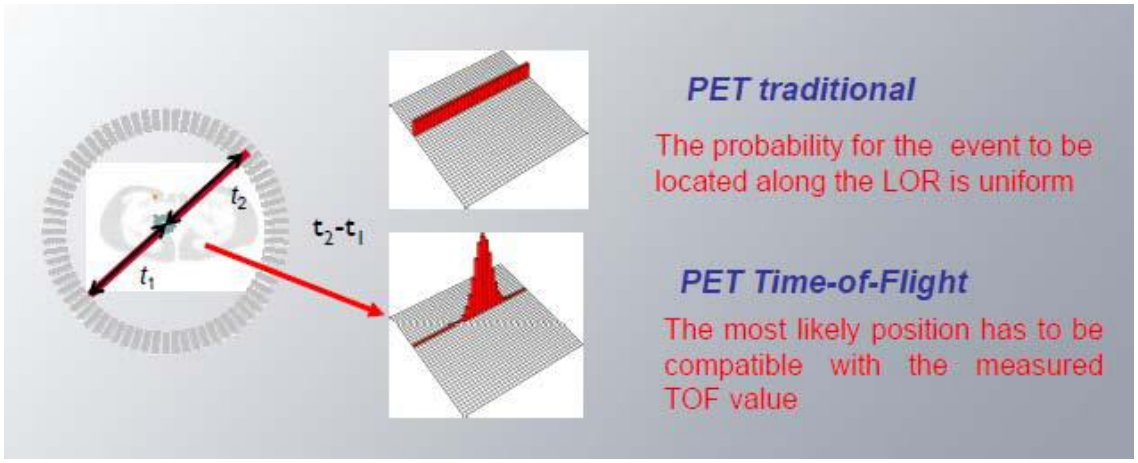

Figure 9: Illustration of the principle of time-of-flight PET measurement (ToF-PET), allowing to increase the image contrast.

These developments, together with the ability to sustain higher data rates, the possibility of real time PET and SPECT images, are enabled by complex, new electronics, even dedicated ASICs, all developed as a result of needs in nuclear physics experiments.

CURRENT TRENDS: Nowadays the combination of more than one imaging modality is preferred over a single modality. Since 20 years ago, PET-CT and SPECT-CT have replaced the single PET or SPECT clinical systems, as the high spatial resolution of X-ray CT images increased several folds the diagnostic capabilities of PET and SPECT images. However, the better contrast in soft tissue and the huge versatility is increasing the interest in combining Magnetic Resonance Imaging (MRI) with PET or SPECT. However, MRI requires large magnetic fields, which are totally incompatible with the old-fashioned photomultiplier vacuum tubes (PMT) employed in traditional PET and SPECT systems. While solid state detectors, such as avalanche photodiodes (APDs) have been at play for decades, these have proven unreliable and difficult to incorporate into stable designs (however, a few commercial systems based on APDs are available). But a newcomer, the Silicon Photomultiplier (SiPM), being marketed regularly less than 10 years ago, is now widely used. They are also solid state detectors, small and less power consuming than PMTs, insensitive to magnetic fields and conventional or digital SiPM [Dam 2013, Schaart 2016] are much easier to use than APDs. The available systems seem to be changing overnight thanks to APDs and SiPMs, and new combined PET/MRI or PET/SPECT systems, as well as PET inserts for MRI scanners, are being announced several times per year.

In the X-ray CT arena, the quest towards multi-energy spectral CT, high quality low-dose imaging is progressing with giant steps. $LaBr_3$ CT systems are being commercialized, offering faster imaging with reduced dose. Indeed, the combination of new scintillators or solid state detectors with powerful tomographic image reconstruction methods is enabling ultra-low-dose, high-quality CT images as well as enhancing the contrast in soft tissues. Moreover, CT scanners using photons of different energies, and/or detectors with spectral (i.e., the ability of disentangling the energy of the X rays detected) capabilities are under heavy research.

The limited scope of this overview does not allow for covering in detail also the new generation of silicon-based, high resolution charged particle and/or photon detectors (like MediPIX and its derivatives). These chips are directly derived from the ones developed to satisfy the needs of high energy and nuclear physics experiments, yet hold the potential to change the way nuclear imaging is performed.

Reverting the original flow of technology transfer from basic nuclear physics to applications in the medical field, nowadays the activities of many nuclear physics groups are receiving a boost thanks to the need to evolve nuclear imaging detectors. Multi-national nuclear physics experiments make it possible to train and shape the best technicians, PhD students, researchers and other experts in technology for nuclear detection. Nuclear physics groups are increasingly aware (although this should be promoted and stimulated) that their work in radiation detector development, simulations, signal processing electronics, and data processing, may enable important new possibilities in nuclear medicine and particle therapy-related imaging. The activities in these two fields are complementary and synergetic. On the one hand, the existing dedicated equipment at nuclear detector laboratories, as well as the related manpower in academia, associated with nuclear physics groups working in international collaborations on nuclear detectors, outnumber by far the very few instrumentation development groups existing in medical schools. Not even the largest hospitals can afford dedicated laboratories for radiation detection and electronics development. While the synergies between the nuclear physics and medical field are outstanding, academia still needs an incentive, and specific combined training programs are still scarce, giving even more emphasis to

initiatives like the MediNet network that brings together groups from both fields, united by their interest in developing state-of-the-art detection tools for medical applications.

SECTION 3: RADIATION QUALITY AND CLINICAL EFFECTS

3.1 Dosimetry, biological effects, treatment

During last decades conventional, i.e., photon therapy (X and γ-rays) of malignant diseases is being replaced by hadron therapy. The main goal of using protons and carbon ions, which is based on their inherent physics properties, is to increase precision in targeting the tumour volume while spearing surrounding healthy tissue and to obtain greater biological effectiveness of the applied doses. Currently, more than 150 000 patients worldwide have been treated by protons or carbon ions in almost 60 hadron therapy centres (Europe, USA, Japan, China, South Africa). About 30 new hadron therapy centres are under construction, mostly in Europe, USA, and Japan but also in India, China, Russia, and Korea. Recently, due to advantages of carbon ions over protons, like higher efficiency in cell inactivation and smaller lateral scattering, they are progressively more used for specific tumours (adenocarcinoma, head and neck, lung, prostate, pancreatic carcinoma and soft tissue sarcoma).

In the case of high linear energy transfer (LET) radiation (protons and carbon ions) the density of the ionization is very intense around the track and multiple damages to the DNA chain are created that cannot be repaired. If LET is low single damages to the DNA chain are more probable which are easier to be repaired. For the tumour cells high LET radiation gives an increased efficiency of killing, while for the neighboring healthy tissue this results in an increased collateral damage (acute effects, late effects and secondary cancer induction).

For many years high energy protons have been successfully used in clinical practice for treating different tumour sites. As described in Section 1, to treat a target volume with a proton beam with a uniform dose, the Bragg peak is spread out obtaining the SOBP. The Bragg peak as well as SOBP have a higher LET than the beam entering the tissue.

3.1.1 The relative biological effectiveness (RBE)

The assessment of radiobiological effects is done through the relative biological effectiveness (RBE). The RBE is not unique but depends on the dose and on the specific biological effects that are investigated.

Protons. Commonly used parameter to compare *in-vitro* the cell inactivation potential of protons to γ-rays is the relative biological effectiveness at 2 Gy, the RBE(2 Gy, γ), defined as the ratio of 2 Gy γ-ray dose and the proton dose producing the same cell inactivation level as that given by 2 Gy of the reference γ-rays. RBE strongly depends on LET. RBE values increase along the SOBP. For tissues, LET reaches its maximum at about 100 keV/µm that corresponds to the proton energy of roughly 70 keV RBE attains its maximum at lower LET values, approximately 40 keV/µm. Since the RBE measures effectiveness of proton dose, with respect to that of γ-rays, for inactivation of irradiated cells it is important to evaluate these values both for malignant growth and normal tissue in order to be able to sterilize the first and not to harm the second type of cells.

Due to energy modulation that is used to produce the SOBP, as the thickness of the modulator increases, the fluence of the SOBP starts falling earlier than in the case of the full energy Bragg curve. Simultaneously, the LET starts earlier sharply to rise. Considering that the dose is the product of LET and fluence, the dose level of the SOBP remains flat because the rise of the LET compensates the drop of fluence. The contribution of the high LET component of the dose increases when moving toward the distal edge of the SOBP as well as toward the end of the range. As a result, the decreasing number of particles produces fewer hits on irradiated cells. Several data

collected *in vitro* show the hits by particles with increasing LET cause more irreparable and less reparable lesions. Consequently, there is a higher killing ability of a smaller number of particles when approaching the end of range, which brings RBE to mount. As a consequence, the depth-dose profile in terms of biological effective dose is different from that in terms of physical dose. Practically, the profile of the biological dose is proportional to the product of RBE and physical dose. This means that along the SOBP the physical dose is flat, while biological moderately increases reaching the peak value at the end of the SOBP, close to the end of range of protons. The results obtained *in vitro* are not translated to clinical proton therapy [Paganetti 2014]. It appears evident that that a standardization of the experimental procedures to reduce the uncertainty of the biological response and optimize the determination of the LET values is a necessary step. The ultimate goal is to implement the results in proton therapy planning. The advantages are evident in particular when organs at risk are located just behind the treated tumour.

Carbon ions. Nowadays therapy of many malignant diseases is done in eleven centers worldwide by irradiations of the tumour target using carbon ions. For carbon beams, due to their nuclear interactions with the atoms in the irradiated medium, nuclear fragmentation is a second process beside the energy loss that determines the depth-dose distribution. Lighter ions created in these nuclear reactions continue their path with approximately the same velocity. Having a lower charge than the primary ion the fragments have a greater penetration, thus creating a dose tail at the distal fall-off part of the Bragg curve. The created fragments are predominantly intermediate to low energy ions of boron, beryllium, lithium, helium with protons being by far the most numerous. Among the fragments there are those that reach distances far beyond the range of the primary carbon beam and deliver their energy in the fragmentation tail. In the region of the Bragg peak and tail, the heterogeneity of ion species and energies produces complex biological effects. The physics and, even more important, the biological properties of these events must be studied extensively. The fragmentation tails ought to be directly included in the treatment planning system in order to guarantee the tumor control and avoid complications in neighboring vital normal tissues. In reality, within the integral effect of carbon beams to the depth-dose distribution one can hardly distinguish the contribution of primary carbon ions from each secondary ion species. However, numerical simulations with Monte-Carlo codes as GEANT4 and FLUKA can provide this information by means of calculating each particle fluence, LET and dose. On the opposite, in the fragmentation tail, that is so crucial for therapy and treatment planning systems one can differ the contribution and the efficiency of each secondary ion species, both experimentally and numerically. Under these conditions radiobiological studies, as well as immunohistochemical investigations that are based on the evaluation of damages induced in DNA, carried out after *in vitro* irradiations of human cell monolayers with different ions, provide necessary data to improve knowledge about the effects of secondary particles in carbon ion therapy.

3.1.2 Ionization and DNA damage

Ionizing radiation acts on the DNA, either directly by inflicting DNA damages, or indirectly by affecting DNA metabolism thus causing damages. The induction of DNA double-strand breaks (DSBs) triggers a number of protective mechanisms including the up regulation of repair pathways, cell cycle arrest and sometimes programmed cell death. DSBs trigger phosphorylation of histone H2AX by forming γ-H2AX foci that appear in cells just a few minutes following irradiation, reach maximum and then decrease. This decline is believed to reflect the kinetics of DNA DSB repair. The interaction of γ-H2AX with other proteins may be important for the activation of cell cycle checkpoints after DNA damage. Using the immunohistochemical method for quantitative and qualitative detection of DNA DSBs in situ it is possible to obtain data about the distribution and geometry of the lesions produced by different ions having high LET.

3.2 Monte Carlo simulations

3.2.1 Introduction: Background and history, from nuclear physics applications to medical physics

In 1947 were proposed for the first time statistical methods to solve neutron diffusion problems in fissionable material, during the same period the general-purpose electronic computer ENIAC was released to compute such problems. It became then possible using different distributions of pseudorandom numbers to explore the behavior of neutron chain reactions in fission devices. Von Neumann and Ulam proposed to simulate neutrons in a spherical geometry where materials were varying with radius. Neutrons were generated isotropically with scattering, absorption and fission cross sections changing with neutron speed in order to determine the distance that a neutron travels before interacting with a nucleus. Since 1957, the first Monte Carlo N-Particle Transport code (MCNP) was developed by Los Alamos National Laboratory to simulate nuclear processes such as fission; this code will be able to simulate interactions involving neutrons, photons, electrons and another 34 different types of particles with more than 2000 heavy ions in its last version MCNP6.

Monte Carlo codes describing macroscopic behavior of particles (from micrometer scale to above) make use of a "condensed-history" technique to simulate collisions along a track. Those collisions along a track are grouped together and their effect (particularly the scattering of particles) is simulated through the so-called "multiple scattering" theory. Regarding their ability to simulate charged particles tracks, Monte Carlo codes can be classified in three classes: in class I codes, energy loss and angular deviations associated to individual interactions are grouped but energy and direction of the primary particle are not affected by the creation of secondary particles. In class II codes, only collisions below a cut off value are grouped together while energy and direction of a primary particle are affected by the production of secondaries. Then, in class III codes all elementary interactions are simulated, it is particularly relevant when studying effect of particles at very low energies (below 10 keV) in sub-cellular geometry (nuclear DNA damage for example).

Nowadays, one can find generalist Monte Carlo codes, developed in different languages, able to simulate the majority of hadrons, muons, electrons, photons and neutrons; this is the case for Geant4 [Allison 2006, Allison 2016, Agostinelli 2003] (written in C++) or Fluka [Ferrari 2001] (written in Fortran) supported by CERN for different experiments (from Large Hadron Collider experiments to neutrino beam studies). Even if Geant4 and Fluka can be used for medical physics purposes, other codes are more dedicated to radioprotection or radiation therapy involving photons and electrons such as EGS4 [Ford 1978] (Electron Gamma Shower, written in Mortran), EGS5 [Hirayama], EGSnrc [Kawrakow 2000] (written in C++), Penelope [Baro 1995] (written in Fortran) or MCNPX [Waters 2005] (written in Fortran), others, such as SHIELD-HIT12A [Bassler 2014] (written in Fortran), are focused on ion therapy research. Finally, the GATE platform [Jan 2004, Jan 2011, Sarrut 2014] (written in C++ and using Geant4 libraries) can be used either for medical imaging or radiation therapy applications (from internal to external radiation therapy and hadron therapy).

While computing time is constantly reduced through the usage of fast computers or clusters or even using GPUs, those codes keep being used in research and are partly modified or adapted to be suited for a clinical use in treatment planning softwares (TPS).

3.2.2 Dedicated Monte Carlo codes for medical physics

Monte Carlo codes have witnessed increased use in radiation therapy, one could say that the most popular Monte Carlo softwares practiced for research purpose in radiation therapy using photons or electrons are MCNP6 [Goorley 2016], BEAMnrc [Rogers 2017] and DOSXYZnrc [Walters] (based on EGSnrc), Penelope and the GATE

platform. All those codes provide similar results regarding macroscopic dosimetry, when dose is calculated in volumes higher than 0.1 mm^3 and for energies higher than 10 keV. Some Monte Carlo codes were modified to include hybrid and faster calculations (also named as variance reduction techniques) of the dose using a Track Length Estimator (TLE) method able to estimate particle fluence considering a track length as a straight-line distance traveled through voxels between successive collisions. However, this technique makes drastic approximations regarding the simulation of secondary particles (electrons) that are not followed so users have to carefully select such a method when the electron range is smaller than the spatial resolution required (voxel size of the CT scan) and if there is no significant radiative energy escape after electron collision in tissues.

During the last ten years, regarding the increasing level of complexity of new radiation therapy treatments using photons and electrons, for example with intensity-modulated arctherapy creating a rotational IMRT using overlapping arcs or when radiations are delivered with a robotic radiosurgery system (known as CyberKnife); treatment planning softwares have to adapt their methodology of calculations to integrate Monte Carlo methods for the precise simulation of electrons through tissue heterogeneities or thin pencil photon beams achieving reasonable computing times. The integrated Monte Carlo codes in TPS for electron and/or photon transport are for example: VMC [Kawrakow 1996], VMC++ [Kawrakow 2000] and XVMC [Fippel 1999] for the XiO and Monaco softwares (Elekta), VMC++ for Raystation software (Raysearch), MMC [Neuenschwander 1995] (Macro Monte Carlo) for the Eclipse-eMC (Varian), PENFAST [Habib 2010] for DosiSoft, XVMC is used in iPlan software (BrainLab), MCDOSE [Ma 2002] is part of the Accuray software (Cyberknife). All of them are derived from research Monte Carlo codes (for example MMC is derived from EGS4, PENFAST from Penelope) proposing the optimization of dedicated radiation transport algorithms, the implementation of variance-reduction techniques and suitable approximations. Most of them use pre-calculated Dose Point Kernels (DPKs) or Pencil Beam Kernels (PBK) and combine them all along the track to generate the dose distribution.

Regarding TPS for proton therapy beams, RayStation (Raysearch), Proton Planning Eclipse (Varian) and lastly ISOgray 4.3 (DOSIsoft) have been developed to compute dose distributions with scattering beams and pencil beam scanning.

Regarding ion beam therapy, Geant4 collaboration provides some example of applications useful to study and assess dose, linear energy transfer (LET) and relative biological effectiveness (RBE) distribution. Inside the open-source toolkit, an advanced example named “hadrontherapy” was developed to perform dosimetric studies that could be also correlated with biological studies. Moreover, it is under developing the possibility to include the DICOM (Digital Imaging and Communications in Medicine) images as target inside the application. In this way, it will be possible to reproduce tissue based on DICOM CT images and every kind of irradiation beam line permitting to evaluate three dimensional dose maps for different beam configurations (e.g. modulators, range shifters, collimator diameters, etc.) in order to choose the best treatment configuration. As a consequence, it is possible to perform more precise dosimetric assessment.

For carbon ions, TPS includes also different biophysical models in order to calculate Relative Biological Effectiveness (RBE) as the high linear energy transfer (LET) is responsible for higher damage to cellular and sub-cellular levels.

3.2.3 Monte Carlo role in radiobiological modeling

To discriminate the physical dose (Gy), ICRU recommends use of the term “RBE-weighted” dose (Gy (RBE)) for biological dose (ICRU-72 2007). Biological dose distribution is expressed as a typical tumor cell response, as defined by the in vitro response of human salivary gland (HSG) tumor cells.

Different radiobiological models have been proposed to predict biological dose: the Carabe-Fernandez et al. model, the Wedenberg et al. model, the Chen and Ahmad model, the Wilkens and Oelfke model, the repair misrepair fixation (RMF) model, the Local Effect Model (LEM) version IV, the Microdosimetric Kinetic model (MKM), the amorphous track based MKM, the track structure model. Three of those have been compared by Giovannini et al [Giovannini 2016] for a spread-out Bragg peak (SOBP) as well as two exemplary clinical cases (single field and two fields) for cranial proton irradiation delivered with pencil-beam scanning (PBS). Authors concluded that simpler models based on the linear-quadratic formalism and LET might already be sufficient to reproduce important RBE dependencies for re-evaluation of plans optimized with the current RBE = 1.1 approximation, agreeing that more experimental evidence was needed to validate the accuracy of the investigated models and their input parameters.

Monte Carlo track structure (MCTS) codes tend to be used also for nanodosimetry (molecular level) by estimating the detailed clustering of individual energy depositions. At such low energies and small dimensions, event-by-event tracking is applied without resorting to condensed history techniques, the final objective being to relate micro- and nanodosimetric quantities to biological endpoints. Examples of codes dedicated to micro and nanodosimetry are quite numerous; some of them achieved convincing developments for the evaluation of radiation therapy outcomes. This is the case for example of the Kurbuc code [Uehara] which provides different models for the transport of electrons (Kurbuc_e covering the energy range between 10 eV and 10 MeV), protons (Kurbuc_p covering the energy range between 1keV and 1 MeV) and heavier ions (Kurbuc_carbon covering the energy range between 1keV/u and 10 MeV/u). With the modelling of specific geometries of biological targets, it becomes possible to simulate DNA damage.

The PARTRAC code [Friedland 2012] proposes different modules able to model radiation physical interactions (for photons, electrons and ions), physico-chemical and chemical stages for the calculation of radiation effects to cells and DNA. Even if those codes demonstrated their ability to reproduce biological outcomes, they are not publicly accessible; following the topical review of El Naqa et al [El Naqa 2012], those codes “did not extend to the level that would be clinically useful for predicting radiotherapy response or for designing clinical oncology trials”.

Up to now, Geant4-DNA [Bernal 2015, Incerti 2010] is the only open-source MCTS code. The accurate modeling of the physical stage relates to the constant development and improvement of physical interaction models; so far, the verification and validation of Geant4-DNA physics processes have been achieved for liquid water concerning radial energy deposition for protons, alpha particles, carbon, silicon and iron ions, stopping powers and ranges of electrons, protons and alpha particles, cross section models for electrons, protons, hydrogen atoms, and alpha particles including their charge states, S values for monoenergetic electrons and for electrons emitted by five isotopes of iodine in liquid water and electron dose point kernels in liquid water. The physico-chemical and chemical stages have been delivered to the community in the Geant4 public release (10.1, December 2014).

3.3 Radiation quality

"The right dose differentiates a poison from a remedy….." - stated Paracelsus already few hundred years ago. It is intuitively understandable that radiation effects in biological systems depend on absorbed dose i.e. quantity of radiation interaction with matter. However, the response of living organisms is also related to temporal pattern of exposure (how quick and in how many fractions the radiation dose is given) and moreover to the spatial, microscopic distribution of ionizations produced by radiation. Those phenomena are particularly intriguing because the same amount of energy transferred to the tissue may produce quite different biological effects.

3.3.1 Stopping power and Linear Energy Transfer concepts

There are several methods to quantify the energy deposition by charged particles. A convenient physical quantity that describes the loss of energy by ionizing particle passing the medium is stopping power. The stopping power of material is defined as the ratio of the differential energy loss for the particle within the material to the corresponding differential path length:

$$S(T) = -\frac{dT}{dx} = n_{ion}\bar{I}$$

where T is the kinetic energy of the charged particle, n_{ion} is the number of electron-ion pairs formed per unit path length, and I denotes the average energy needed to ionize an atom in the medium. For charged particles, *S* increases as the particle energy decreases.

The classical expression that describes the specific energy loss is known as the Bethe formula.

$$S(T) = \frac{4\pi Q^2 e^2 nZ}{m\beta^2 c^2}\left[ln\left(\frac{2mc^2\gamma^2\beta^2}{\bar{I}}\right) - \beta^2\right]$$

In this expression, *m* is the rest mass of the electron, β equals to the ratio *v/c* between the particle's velocity and the speed of light, γ is the Lorentz factor of the particle, *Q* equals to its charge, *Z* is the atomic number of the medium and n is the atoms density in the volume. For nonrelativistic particles (heavy charged particles are mostly nonrelativistic), d*T*/dx is dependent on $1/v^2$. This behaviour can be explained by the longer time the slow charged particle spends passing atom orbitals. This equation takes into account only the ionization losses. In addition a small amount of energy is lost by emission of electromagnetic radiation (bremsstrahlung). The stopping power due to the electronic collision is called Linear Energy Transfer, LET in particular in the framework of radiation protection and medical use of radiations. Figure 10 displays the total stopping power for protons and α particles in water as a function of the particle energy per nucleon.

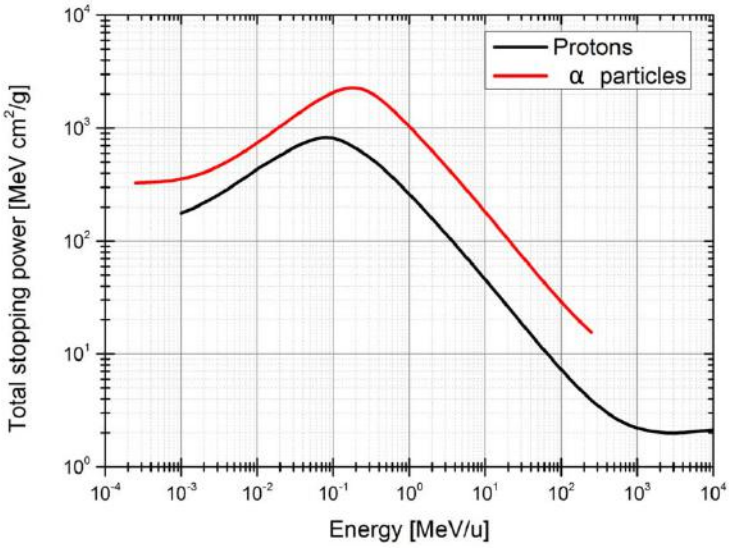

Figure 10: Graph of the total stopping power for protons and alpha ions in water, versus particle energy per nucleon. The maximum of the total stopping curve typically occurs at energies of the order of 0,1 MeV per nucleon for protons and 0,2 MeV per nucleon for alpha particles. Beyond the maximum, stopping power decreases ap-

proximately like $1/v^2$ with increasing particle velocity v, but after a minimum, it increases again [https://physics.nist.gov/PhysRefData/Star].

3.3.2 Stopping power and Linear Energy Transfer in particle therapy

In cancer therapy the term radiation quality is used to describe the source and properties of radiation beams, in particular with regard to type and energy of radiation e.g. 6 MV X-rays, 250 MeV protons, 1.25 MeV photons etc. In microdosimetry the term radiation quality is rather related to the microscopic pattern of energy deposition events. For accelerated ions, like protons or carbon ions, the energy is densely released and concentrated along the track of the particle, mostly at the distances of several dozen of nanometers from the ion path. Within the central part of the track (track core) energy per unit mass (dose) may be as high as thousands of Joules per kilogram. If the track passes through a sensitive biological site such as the DNA structure, it will be destroyed with high probability. Outside the track there are practically no ionizations and dose is close to zero. Photons, which interact with matter and produce sparsely ionizing secondary electrons, lead to much more uniform energy deposition.

Since these characteristics are the same for all particles of a certain species and energy, we can give the general definition of the radiation quality stating that it is the type and energy spectrum of each radiation type in a specific point. The usual ways in which the radiation quality is specified is via linear energy transfer (LET) values, or via microdosimetry quantities. The LET spectra are generally the computational results (e.g. Monte Carlo simulations), while microdosimetry spectra are collected experimentally, using a detector with (simulated) size of the order of one micrometer. Specifying the radiation quality using the mean value of LET simplifies the description of an irradiated field, but also omits important information e. g. RBE value is not the same for different ions having the same LET.

Several in-vitro studies show a significantly enhanced RBE value at the end of the ion path. It is frequently claimed that this enhancement has no influence in the clinics what leads to situation when that treatment planning systems are not taking into account radiation quality changes. Therefore, it needs to be elucidated how this serious discrepancy between the in-vitro results and the clinical trials results can be explained and to identify the situations where the radiation quality changes (e. g. LET value changes) might have strong influence.

3.4. Adaptations of sizes and targets types in radiation quality

As explained in section 3.3.2, the experimental evidence that radiobiological effects, for the same absorbed dose, are different when radiations of different kinds and energy are used, led to the concept of radiation quality. Namely, the absorbed dose has a quality, which has to be specified with the multiplicative factor described in sections 3.1.1 and 3.3.1 as RBE. When in radiation therapy high-energy photons are used, the RBE is generally taken as 1.0. When fast protons are used, the clinical RBE is taken as 1.1 [IAEA-ICRU 2006, Paganetti 2014]. When fast neutrons are used, the RBE depends on the neutron energy-spectrum. When high-energy carbon ions are used, the RBE has been observed to change with the depth. The carbon-ion therapy centre of Chiba in Japan for passively spread-out beams (at an irradiation depth equivalent of 16 cm of water and a 6 centimetres spread-out to cover the area where the tumour is) considered in the middle of the SOBP a clinical RBE of 3, and RBE values varying between 2.1 close to the beam entrance to 3.4 at the beam end [IAEA-ICRU 2008]. The physical basis of the radiation quality is still a matter of research. Different proposals have been submitted, with the so-called microdosimetry approach being the most fruitful.

3.4.1. The microdosimetry model

The biological action of radiations initiates with the radiation damage of biological structures, which have finite size. Therefore, let us move from the point of view of the site when the biological sample absorbs the dose *D*. It is

reasonable to assume that the biological damage is a function of the energy imparted ε in the biological site. However, depending on the site size, ε is due to one or more particles crossing or licking the site. Hence, sites of different size experience different modalities of energy absorption. When the site is relatively large, the ε-value is due to several particles. Some of them cross the site without imparting any energy. They give rise to ε_0 events, the size of which is 0. Other particles releases energy inside the site; we call ε_s the no-0 event, that a single particle gives rise to. Different particles give rise to different ε_s-value, since the particle-matter interaction is intrinsically stochastic for quantum mechanical reasons. Therefore, the ε_s-values fluctuate around their average. The ε_s spectrum is the conditional probability (so is the probability to have an event when ε_0 events are excluded) to have in the site a given ε-value due to a single particle only. A fast detector, a gas proportional counter or a solid-state detector, can measure the ε_s spectrum, hence the probability to have a given ε_s event in the detector sensitive volume.

The total energy imparted ε in the site is the sum of all the ε_s single-events the ε_0 events and also the multi-events, the ε-value fluctuates, being different from site to site. The ratio of ε on *m* is called *specific energy z*, where *m* is the site mass. The physical dimensions of *z* are those ones of the absorbed dose, but the *z*-value fluctuates, while the absorbed dose does not, since it is the fluctuation's mean value. If we exclude from ε the zero events, we obtain the quantity z^*, that means the specific energy in a site that experiences at least one ε_s-event (*critical site*). The ratio of the mean value $\overline{\varepsilon}$ of the imparted energy on *m*, namely $\overline{z}$, is the usual absorbed dose *D,* when both the target and the radiation field are uniform. Similarly, the mean value of z^* is $\overline{z}^*$, namely the absorbed dose in a *critical site*. This short description of the radiation-matter interaction shows that the absorbed dose *D* is only related to the mean value of the imparted energy. The *D*-value is a look from afar of the interaction, when the microscopic sites vanish and consequently *D* does not depend on the site size (when it is uniform in the sample, of course). However, a closer view of the interaction tells us another story: a varied landscape that changes with the absorbed dose, with the site size and with the radiation quality.

When the site is as small as some critical biological structures (microdosimetric dimensions or less) and the dose is of the order of 0.1 Gy, no more than 1 particle crosses the site. Decreasing the site size, ε_0 events are more and more numerous. Obviously, ε_0 events do not cause any biological action in the site. Only ε_s events and multi-events contribute to the biological action.

Based on these concepts, the microdosimetric model assumes that only the single-event imparted-energy density ε_s/m is meaningful for the radiobiological action, since multi-events are rare in the critical biological structures, which are very small. The ε_s/m ratio is called *specific energy of single event* z_1. z_1-value fluctuates around its mean value $\overline{z}_{1F}$. This average has the same physical dimensions of the absorbed dose *D,* but its value is different both from *D* and $\overline{z}^*$. If the site shape is known, the ratio $\varepsilon_s/\overline{l}$, where $\overline{l}$ is the site mean-chord length, defines the physical quantity *y*, called *lineal energy*, which has the same physical dimensions of LET (see § 3.3.2), but its value varies from site to site (similarly to z_1), fluctuating around its mean value $\overline{y}_F$. For a given site, *y* is proportional to z_1.

3.4.2 Microdosimetry and radiation quality

At the Antoine-Lacassagne centre of Nice (France), ocular-melanoma tumours are treated with 62 MeV proton beams.

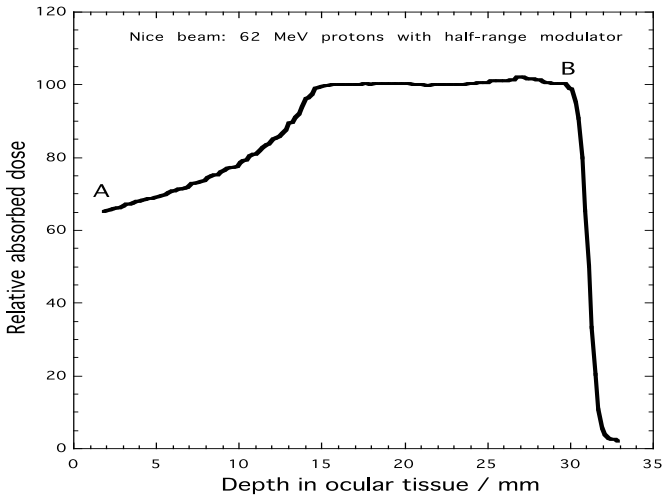

Figure 11: The SOBP (spread-out Bragg-peak) used at the Nice therapeutic Centre to treat ocular tumours. Letters A and B point out two positions where microdosimetric measurements were performed.

In Figure 11 the relative dose absorbed in a therapeutic plan is plotted against different depths in tissue. With the use of a range modulator the dose profile is made flat just inside the depth range to be treated obtaining the spread out Bragg peak described in Section 1.

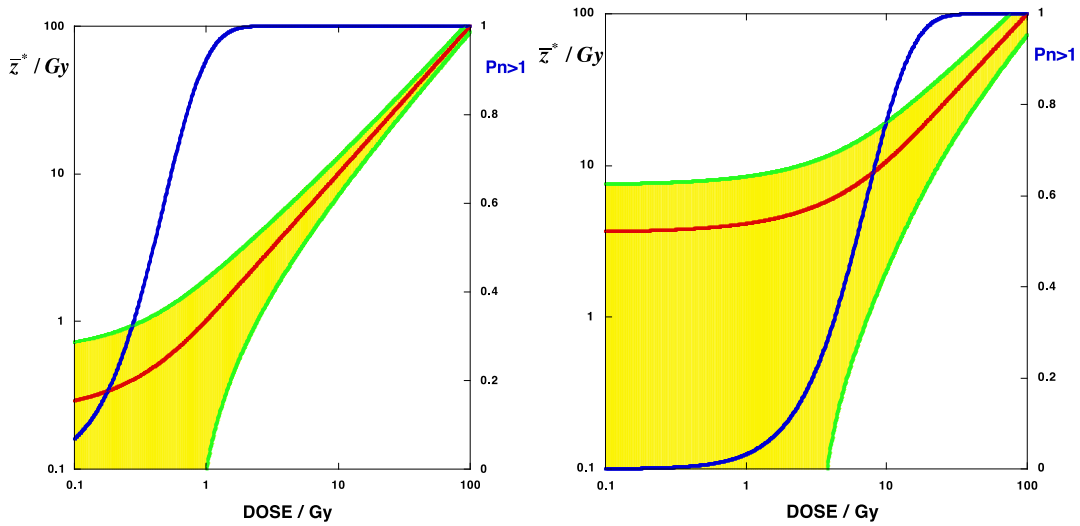

Figure 12: Red line: mean specific energy in 1 µm critical site against the absorbed dose of the 62 MeV proton beam of Nice therapeutic centre. Green lines: ± 1 standard deviation of the mean specific energy. Yellow area: z*-values fluctuations in between. Blue line: probability to have more than 1 event in the site, against the absorbed dose. Left-side figure: from experimental data taken in position A of figure 11. Right-side figure: from experimental data taken in position B of figure 11. See text.

The radiation quality in position B is different from that in position A, since the proton beam energy is different. Figure 12 illustrates such a difference from the point of view of a site of 1 µm of diameter at increasing absorbed dose. At the proximal edge, when protons are still very fast, the majority of sites experience only one ε_s event

(93% of all) at low dose (0.1 Gy). Increasing the absorbed dose, more and more sites are hit. At 2 Gy all the sites experience more than 1 ε_s event: we enter into the multi-event region. When all the sites undergo more than 1 event, $\overline{z}^* \approx D$. However, different sites can still experience much higher z^*-values (yellow region). At low absorbed dose, $\overline{z}^* \neq D$, since $\overline{z}^*$ becomes constant and equal to $\overline{z}_{1F}$. This is the region ($D \lesssim 0.1$ Gy) where single-event spectra become necessary to describe the interaction of radiation-matter in microscopic sites. At the end of the spread-out Bragg-peak (SOBP), more than 30 Gy are necessary to fill all the sites with more than 1 ε_s event. The region where the single-event is dominant is for D $\lesssim$ 1 Gy.

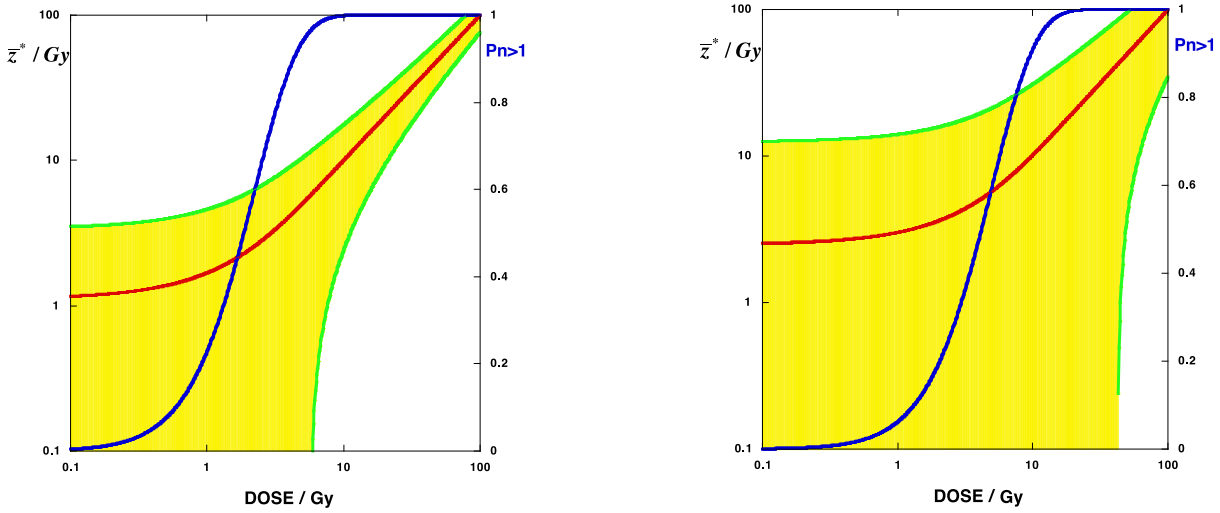

Figure 13: Red line: mean specific energy in 1 µm critical site against the absorbed dose of the 189.5 MeV/u carbon-ion beam of the CNAO therapeutic centre. Green lines: ± 1 standard deviation of the mean specific energy. Yellow area: z*-values fluctuations in between. Blue line: probability to have more than 1 event in the site, against the absorbed dose. Left-side figure: from experimental data taken in the proximal edge (beam entrance). Right-side figure: from experimental data taken at the SOBP end. See text.

Similarly to figure 12, figure 13 shows specific-energy in *critical sites* changes, at increasing absorbed dose for the 189.5 MeV/u carbon-ion beam, which is used at the CNAO therapeutic centre. At the proximal edge, the mean specific energy and its fluctuations are similar to those of protons at the end of the SOBP: ~ 10 Gy are necessary to saturate all the sites with at least 1 ε_s event and the single-event interaction dominates for $D \lesssim 1$ Gy. At deeper depth, the carbon-ion quality changes. Now, about 20 Gy are necessary to saturate all the sites with at least 1 ε_s event, while the single-event interaction dominates for $D \lesssim 2$ Gy. These values are similar to those of protons at the SOBP end, but the z^* fluctuations are larger for carbon ions.

3.4.3 The role of ε_s fluctuations at different site sizes.

Both for protons and carbon ions, the region where $\overline{z}^*$ becomes constant and equal to $\overline{z}_{1F}$, namely the single-event region, extends towards higher absorbed doses as the site size decreases. For sites less than 0.1 µm of size, the single-event region upper limit approaches 100 Gy also for the so-called low-LET radiations. On the contrary, for site sizes larger than 1 µm the single-event region upper limit is reached at smaller dose values. For site sizes close to 100 µm, the single-event region survives only for very small absorbed-dose values. Hence, the ordinary mean quantities (absorbed dose, stopping power, LET) describe sufficiently well the interaction features in these "macroscopic" sites, also for high-LET particles, the z^* fluctuations play a minor role.

3.5 Nuclear measurements and medical applications: repeatability and reproducibility

3.5.1 Repeatability and reproducibility

Since their discovery, the use of radiation in medical application has produced undoubtedly improvement both in the diagnosis and the treatment of several diseases. As any other medical process, the delivery of radiation for diagnostic or therapy purpose must be carried out under specific and strict requirements, a general reference is the Technical Report TRS 398 published by the International Atomic Energy [IAEA 398]. In simple words, the whole process from planning to radiation delivery, has to be monitored in regards of its quality, accuracy, repeatability and reproducibility.

The reason for such an approach is twofold. First, for the safety of the patient and the operators. Our goal is maximizing the effects reducing the dose level –the ALARA principle applies, meaning "As Low As reasonably Achievable—and therefore the side effects. Second, to make the treatment conditions under a common standard in order to allow multi-centre clinical studies.

Such a system of quality assurance is widely established in clinical routine by means of a well-defined quality control schedule, which periodicity depends on the criticity of the parameters to monitor. Their aim is to guarantee a uniformity of treatment to all patients with the same level of accuracy and precision. The focus of the quality assurance is therefore on the treatment and not on the patient.

In a pre-clinical experimental environment, where the goal is discovering new strategies and test new treatment approaches, the situation is slightly different. Here, all the possible degrees of freedom with the exception of the compliance to ethical issues on animal use, can be implemented without the limitation to apply a pre-defined protocol. On the other hand, the amount of physics variables used to measure and physiological process to monitor, is extremely high. Moreover, due to intrinsic physiologic variability, the behaviour of similar subjects can vary drastically even under the same conditions.

In these regards, it is absolutely necessary to define a system to guarantee on one hand the reproducibility of the treatment, on the other one the uniformity of physiological conditions of the subjects. If we compare to a routine patient treatment, here the focus is both on the treatment and on the patients.

Let us clarify this with an example. Assume that we are performing an experiment to test new tumor treatments. We have three groups of mice both affected with tumor glioma located near the brain stem. The first group will be treated with a new drug, the second with carbon-ions, and the third with a combination of both drug and carbon-ions. Our goal is to detect which of the three treatments is more efficient in terms of tumor control and side-effects to surrounding tissue. In principle, we do not know what will happen and our aim is to make correlations between treatment type and physiological results. In this case, not only the treatment must be monitored to guarantee repeatability and reproducibility, but also all the physiological conditions of the mice must be under control, e.g. body temperature, oxygen saturation, stress level, tumor stage, tissue pH, etc. The reason is that each of these factors can have a strong influence on the results. For example, a higher body temperature can induce vasodilatation and therefore a higher flow of drug to tumor but also to healthy organs.

The great advantage of an experimental set-up is the possibility to mix-up variables in order to find new correlations among them. Such correlations can explain details of a physiological process that in turn become the final target for developing new therapies. Moreover, working in-vivo with animals or in-vitro with biological tissues, the time needed for an experiment can be abundantly increased allowing the acquisition of more and more features.

These high degrees of freedom and variability introduce risks in terms of robustness, false positive or false negative, and clearly increase the level of background. Data analysis, is therefore a critical step in the process, which must be performed in a rigorous way from the statistical point of view.

A common approach is to perform an experiment in two steps. First a pilot study with a small number of subjects in advance, in order to evaluate the variability of the features to measure. Second, the real experiment with a number of subjects accurately evaluated based on the results of the pilot study.

3.2.1 New opportunities offered by modern technology

As of today, the never-ending development of nuclear application in the medical field is offering more and more opportunities either in diagnosis or treatment or both (theragnostics). From the technological perspective, modern microdosimeters and nanodosimeters allow for the measuring of dose and specifying radiation quality in a very small volume with online measurements. Moreover, modern diagnostic techniques such as Positron Emission Tomography (PET) and Magnetic Resonance Imaging (MRI) allow acquiring physiological features in-vivo and in real time. These data are ideal to develop mathematical models of physiological processes because they are direct measurement of the process in-vivo and not a reproduction in-vitro. More specifically, the same approach can be used to monitor the efficacy of the radiation-therapy treatment, where the model to study is the regression of tumor tissue.

Combining the microscopic results from the in-vivo microdosimetry together with the imaging readout from PET and MRI, it is possible in principle to define the efficacy of the treatment and minimize the damage to the healthy tissue at a microscopic level for each patient. These concepts are beyond the standard approach in clinical routine, but they can be easily translated from the research environment to clinics in a reasonable period of time.

CONCLUSION

This document is meant to demonstrate the close relation between basic nuclear (and atomic) concepts and their translation into the field of medical physics and clinical application. Ever since the discovery of X-rays and radioactivity, both of them quickly being translated into the medical field, cross-fertilization between nuclear physics and related technology developments fostered the development of medical physics and medical applications, from imaging and diagnostics to therapeutic applications as outlined in the previous sections:

- the concepts of electromagnetic radiation and the characteristics of photon-matter interaction processes, together with radioactive decay modes and their detectable signatures as well as the behavior of charges and spins in magnetic fields, giving rise to a broad scope of highly sensitive diagnostics (imaging) technologies nowadays common practice in medicine,
- energy deposition in matter allowing for tumor treatment, based on the achievements of accelerator technology translated from basic research to industrial maturity for clinical use,
- ion optical principles applied to (therapeutic) particle beam focusing or bending
- and last but not least the application of laser light in a plethora of medical applications.

Moreover, in all of these fields the initial motivation for research and development, rooted in fundamental scientific interest, finally led to a smooth transfer of technologies into the medical application sector. This holds for large equipment like accelerators, which started out as purely research-driven devices of partly impressively large dimensions, while in the meanwhile application-based industrial developments have led to a stunning reduction

of dimensions as well as costs for medically relevant particle and photon-generating accelerators. While the term 'linac' in the realm of basic elementary particle physics is often associated with kilometer-long devices like SLAC at Stanford or the potentially future 20 km-long and 20 billion dollar costly International Linear Collider ILC, a 'linac' in medical physics terminology refers to a compact machine that fits into a small container of the size of a shoe box if it is used for diagnostics, or of the size of a suitcase if it is used for therapy and can be found even in radiological practices , yet providing MeV-range photons for radiotherapy. The same holds for detectors and their signal processing and data acquisition electronics.

To a large extent synergies have been exploited to harvest the benefits of basic research for the field of medical physics and (pre-)clinical applications. This was only made possible by an open and unbiased institutional cooperation between fundamental research institutions and application-driven facilities or research teams within the research facilities. Prototype hadron therapy facilities like the one operated for several years at GSI before translating the assembled knowledge into a dedicated and hospital-based therapy center demonstrate this beneficial cooperation. Along the same line the production of medical isotopes at research centers (and nuclear research reactors) can be named, often operated in time-sharing mode of the available beamtime at accelerator-based facilities (isotope production during clinical working hours and research during nights and weekends).

Commercialization and standardization of key technologies, via a fruitful cooperation between academia and industry, play a key role in the process of advancing the impact of physical concepts in the medical field.

This approach makes possible the translation from conceptual physics studies into mature industrial products in the fields of accelerators, detectors and electronics components, accompanied by suitable computational tools, via a fruitful cooperation between academia and industry play a key role in the process of advancing the impact of physical concepts in the medical field and ultimately to the society.

Along with the continuously softening borderline between pure and applied physical sciences goes an interdisciplinary cooperation between medical doctors and medical physicists in clinical practice, assisted by professional networks like the Particle Therapy Cooperation Group (PTCOG) in the worldwide growing field of hadron therapy, national and international professional societies of Medical Physicists or last but not least also networking activities like the MediNet network within the European ENSAR2 Integrating Initiative, bringing together research physicists, medical physics practitioners at clinical centers.

The present document could give only a glimpse into the wide range of ongoing activities towards applying basic physical concepts, here in particular atomic and nuclear ones, while aiming at responding to pressing societal needs.

REFERENCES AND APPLICABLE DOCUMENTS

Agostinelli S, et al. Geant4 - a simulation toolkit. Nucl Instruments Methods Phys Res Sect A Accel Spectrometers, Detect Assoc Equip. 2003;506: 250–303. doi:10.1016/S0168-9002(03)01368-8

Allison J, Amako K, Apostolakis J, Araujo H, Arce Dubois P, Asai M, et al. Geant4 developments and applications. IEEE Trans Nucl Sci. 2006;53: 270–278. doi:10.1109/TNS.2006.869826

Allison J, Amako K, Apostolakis J, Arce P, Asai M, Aso T, et al. Recent developments in G eant 4. Nucl Instruments Methods Phys Res Sect A Accel Spectrometers, Detect Assoc Equip. 2016;835: 186–225. doi:10.1016/j.nima.2016.06.125

Baro J, Sempau J, Fernandez-Varea JM, Salvat F. PENELOPE: an algorithm for Monte Carlo simulation of the penetration and energy loss of electrons and positrons in matter. Nucl Instruments Methods Phys Res Sect B Beam Interact with Mater Atoms. 1995;100: 31–46.

Bassler N, Hansen DC, Lühr A, Thomsen B, Petersen JB, Sobolevsky N. SHIELD-HIT12A - a Monte Carlo particle transport program for ion therapy research. J Phys Conf Ser. IOP Publishing; 2014;489: 12004. doi:10.1088/1742-6596/489/1/012004

Bernal MA, Bordage MC, Brown JMC, Davídková M, Delage E, El Bitar Z, et al. Track structure modeling in liquid water: A review of the Geant4-DNA very low energy extension of the Geant4 Monte Carlo simulation toolkit. Phys Medica. 2015; 1–14. doi:10.1016/j.ejmp.2015.10.087

Bisogni M, Attili A, Battistoni G, Belcari N, Cerello P, Coli S, et al. INSIDE in-beam positron emission tomography system for particle range monitoring in hadrontherapy. Journal of Medical Imaging 2017;4

Dam, H.T. van, Borghi, G., Seifert, S., Schaart, D.R., 2013. Sub-200 ps CRT in monolithic scintillator PET detectors using digital SiPM arrays and maximum likelihood interaction time estimation. Phys. Med. Biol. 58, 3243. doi:10.1088/0031-9155/58/10/3243

El Naqa I, Pater P, Seuntjens J. Monte Carlo role in radiobiological modelling of radiotherapy outcomes. Phys Med Biol. 2012;57: R75-97. doi:10.1088/0031-9155/57/11/R75

Ferrari A, Ranft J, Sala PR. The FLUKA radiation transport code and its use for space problems. Phys medica PM an Int J devoted to Appl Phys to Med Biol Off J Ital Assoc Biomed Phys AIFB. 2001;17 Suppl 1: 72–80. Available: http://www.ncbi.nlm.nih.gov/pubmed/11770541

Fippel M. Fast Monte Carlo dose calculation for photon beams based on the VMC electron algorithm. Med Phys. 1999;26: 1466–1475.

Fontana, M. et al, to be published in Acta Physica Polonica B, 48, n°10, Proceedings of the 2nd Jagiellonian Symposium on Fundamental and Applied Subatomic Physics, Kraków, Poland, June 4–9, 2017.

Ford RL, Nelson WR. The EGS Code System: Computer Programs for the Monte Carlo Simulation of Electromagnetic Cascade Showers. SLAC-210; 1978.

Friedland W, Kundrát P, Jacob P. Stochastic modelling of DSB repair after photon and ion irradiation. Int J Radiat Biol. 2012;88: 129–36. doi:10.3109/09553002.2011.611404

Giovannini G, Böhlen T, Cabal G, Bauer J, Tessonnier T, Frey K, et al. Variable RBE in proton therapy: comparison of different model predictions and their influence on clinical-like scenarios. Radiat Oncol. Radiation Oncology; 2016;11: 68. doi:10.1186/s13014-016-0642-6

Goorley T, James M, Booth T, Brown F, Bull J, Cox LJ, et al. Features of MCNP6. Ann Nucl Energy. 2016;87: 772–783. doi:10.1016/j.anucene.2015.02.020

Habib B, Poumarede B, Tola F, Barthe J. Evaluation of PENFAST – A fast Monte Carlo code for dose calculations in photon and electron radiotherapy treatment planning. Phys Medica. 2010;26: 17–25. doi:10.1016/j.ejmp.2009.03.002

Haettner E., et al.,2006. “Experimental fragmentation studies with C-12 therapy beams”. In: Radiation Protection Dosimetry 122, 485– 487.

Hirayama H, Namito Y, Bielajew AF, Wilderman SJ, Nelson WR. The EGS5 Code System. Available: http://slac.stanford.edu/cgi-wrap/getdoc/slac-r-730.pdf

Hueso-González, F., Enghardt, W., Fiedler, F., Golnik, C., Janssens, G., Petzoldt, J., Prieels, D., Priegnitz, M., Römer, K.E., Smeets, J., Stappen, F.V., Wagner, A., Pausch, G., 2015. First test of the prompt gamma ray timing method with heterogeneous targets at a clinical proton therapy facility. Phys. Med. Biol. 60, 6247. doi:10.1088/0031-9155/60/16/6247

Hueso-González, F., Golnik, C., Berthel, M., Dreyer, A., Enghardt, W., Fiedler, F., Heidel, K., Kormoll, T., Rohling, H., Schöne, S., Schwengner, R., Wagner, A., Pausch, G., 2014. Test of Compton camera components for prompt gamma imaging at the ELBE bremsstrahlung beam. J. Instrum. 9, P05002. doi:10.1088/1748-0221/9/05/P05002

IAEA-ICRU, International Atomic Energy Agency and International Commission on Radiation Units and Measurements , Relative Biological Effectiveness in Ion Beam Therapy, Technical Reports Series No. 461, Jointly sponsored by the IAEA and ICRU, Vienna 2008,

IAEA-ICRU, International Atomic Energy Agency and International Commission on Radiation Units and Measurements ,Dose Reporting in Ion Beam Therapy, Technical Document No. 1560, Vienna 2008

Incerti S, Ivanchenko A, Karamitros M, Mantero A, Moretto P, Tran HN, et al. Comparison of GEANT4 very low energy cross section models with experimental data in water. Med Phys. American Association of Physicists in Medicine; 2010;37: 4692–4708. Available: http://link.aip.org/link/MPHYA6/v37/i9/p4692/s1&Agg=doi

Jan S, Benoit D, Becheva E, Carlier T, Cassol F, Descourt P, et al. GATE V6: a major enhancement of the GATE simulation platform enabling modelling of CT and radiotherapy. Phys Med Biol. IOP Publishing; 2011;56: 881–901.

Jan S, Santin G, Strul D, Staelens S, Assié K, Autret D, et al. GATE: a simulation toolkit for PET and SPECT. Phys Med Biol. 2004;49: 4543–4561. Available: http://www.pubmedcentral.nih.gov/articlerender.fcgi?artid=3267383&tool=pmcentrez&rendertype=abstract

Kawrakow I, Fippel M, Friedrich K. 3D electron dose calculation using a Voxel based Monte Carlo algorithm (VMC). Med Phys. 1996;23: 445–457.

Kawrakow I, Fippel M. VMC++, a MC algorithm optimized for electron and photon beam dose calculations for RTP. Enderle JD, editor. Proceedings of the 22nd Annual International Conference of the IEEE Engineering in Medicine and Biology Society Cat No00CH37143 IEEE; 2000 pp. 1490–1493. doi:10.1109/IEMBS.2000.898024

Kawrakow I. Accurate condensed history Monte Carlo simulation of electron transport. I. EGSnrc, the new EGS4 version. Med Phys. 2000;27: 485–498.

Krimmer, J., Ley, J.-L., Abellan, C., Cachemiche, J.-P., Caponetto, L., Chen, X., Dahoumane, M., Dauvergne, D., Freud, N., Joly, B., Lambert, D., Lestand, L., Létang, J.M., Magne, M., Mathez, H., Maxim, V., Montarou, G., Morel, C., Pinto, M., Ray, C., Reithinger, V., Testa, E., Zoccarato, Y., 2015. Development of a Compton camera for medical applications based on silicon strip and scintillation detectors. Nucl. Instrum. Methods Phys. Res. Sect. Accel. Spectrometers Detect. Assoc. Equip., New Developments in Photodetection NDIP14 787, 98–101. doi:10.1016/j.nima.2014.11.042

Krimmer, J. et al., 2017, to be published in Nuclear Instruments and Methods in Physics Research A, http://dx.doi.org/10.1016/j.nima.2017.07.063

Ma CM, Li JS, Pawlicki T, Jiang SB, Deng J, Lee MC, et al. A Monte Carlo dose calculation tool for radiotherapy treatment planning. Phys Med Biol. 2002;47: 1671–89. Available: http://www.ncbi.nlm.nih.gov/pubmed/12069086

Mairani A., 2007."Nucleus-nucleus interaction modelling and application in ion therapy treatment planning". In: Scientifica Acta 1 N 1, 129–132.

Marafini M, Attili A, Battistoni G, Belcar N., Bisogni MG, Camarlinghi N et al., The INSIDE Project: Innovative Solutions for In-Beam Dosimetry in Hadrontherapy. Acta Physica Polonica A127 (2015) 1465.

McMillan, E., 1952. US patent 2615129, Synchro-Cyclotron, issued 1952-10-21.

Neuenschwander H, Mackie TR, Reckwerdt PJ. MMC--a high-performance Monte Carlo code for electron beam treatment planning. Phys Med Biol. 1995;40: 543–574.

Paganetti H., Relative biological effectiveness (RBE) values for proton beam therapy. Variations as a function of biological endpoint, dose, and linear energy transfer, Phys. Med. Biol. 59 (2014) R419–R472

Polf, J.C., Avery, S., Mackin, D.S., Beddar, S., 2015. Imaging of prompt gamma rays emitted during delivery of clinical proton beams with a Compton camera: feasibility studies for range verification. Phys. Med. Biol. 60, 7085. doi:10.1088/0031-9155/60/18/7085

Richter, C., Pausch, G., Barczyk, S., Priegnitz, M., Keitz, I., Thiele, J., Smeets, J., Stappen, F.V., Bombelli, L., Fiorini, C., Hotoiu, L., Perali, I., Prieels, D., Enghardt, W., Baumann, M., 2016. First clinical application of a prompt gamma based in vivo proton range verification system. Radiother. Oncol. 118, 232–237. doi:10.1016/j.radonc.2016.01.004

Roellinghoff, F., Benilov, A., Dauvergne, D., Dedes, G., Freud, N., Janssens, G., Krimmer, J., Létang, J.M., Pinto, M., Prieels, D., Ray, C., Smeets, J., Stichelbaut, F., Testa, E., 2014. Real-time proton beam range monitoring by means of prompt-gamma detection with a collimated camera. Phys. Med. Biol. 59, 1327–1338.

Rogers DWO, Walters B, Kawrakow I. BEAMnrc Users Manual. 2017; Available: https://nrc-cnrc.github.io/EGSnrc/doc/pirs509a-beamnrc.pdf

Sarrut D, Bardiès M, Boussion N, Freud N, Jan S, Létang J-M, et al. A review of the use and potential of the GATE Monte Carlo simulation code for radiation therapy and dosimetry applications. Med Phys. 2014;41: 64301. doi:10.1118/1.4871617

Schaart, D.R., Charbon E., Frach T., Schulz V., "Advances in Digital SiPMs and their Application in Biomedical Imaging," Nuclear Instruments and Methods in Physics Research A 809, 31-52, 2016.

Solevi, P., Muñoz, E., Solaz, C., Trovato, M., Dendooven, P., Gillam, J.E., Carlos Lacasta, Oliver, J.F., Rafecas, M., Torres-Espallardo, I., Llosá, G., 2016. Performance of MACACO Compton telescope for ion-beam therapy monitoring: first test with proton beams. Phys. Med. Biol. 61, 5149. doi:10.1088/0031-9155/61/14/5149

Thirolf, P.G., Aldawood, S., Böhmer, M., Bortfeldt, J., Castelhano, I., Dedes, G., Fiedler, F., Gernhäuser, R., Golnik, C., Helmbrecht, S., Hueso-González, F., Kolff, H. v.d., Kormoll, T., Lang, C., Liprandi, S., Lutter, R., Marinšek, T., Maier, L., Pausch, G., Petzoldt, J., Römer, K., Schaart, D., Parodi, K., 2016. A Compton camera prototype for prompt gamma medical imaging. EPJ Web Conf. 117, 5005. doi:10.1051/epjconf/201611705005

Uehara, Nikjoo H. KURBUC - a Monte Carlo electron track structure code in the range 10-10 MeV in water. Int J Radiat Biol. 1994;65. Available: https://www.har.mrc.ac.uk/kurbuc-monte-carlo-electron-track-structure-code-range-10-10-mev-water

Veksler, V.I., 1944. A New Method of Accelerating Relativistic Particles. Doklady Akad. Nauk SSSR (Proceedings of the USSR Academy of Sciences) (in Russian) 43, pp 346–348.

Verellen, D. et al., 2007. Innovations in image-guided radiotherapy, Nature Reviews 7, pp. 949-960.

Walters B, Kawrakow I, Rogers DWO. DOSXYZnrc Users Manual. Source. NRC; 2011;794. Available: http://irs.inms.nrc.ca/software/beamnrc-V4-2.3.1/documentation/pirs794.pdf

Waters L S, Hendricks J MG. MCNPX version 2.5.0. Los Alamos: Los Alamos National Laboratory; 2005.